An NFFT based approach to the efficient computation of dipole-dipole interactions under various periodic boundary conditions

Franziska Nestler

We present an efficient method to compute the electrostatic fields, torques and forces in dipolar systems, which is based on the fast Fourier transform for nonequispaced data (NFFT). We consider 3d-periodic, 2d-periodic, 1d-periodic as well as 0d-periodic (open) boundary conditions. The method is based on the corresponding Ewald formulas, which immediately lead to an efficient algorithm only in the 3d-periodic case. In the other cases we apply the NFFT based fast summation in order to approximate the contributions of the nonperiodic dimensions in Fourier space. This is done by regularizing or periodizing the involved functions, which depend on the distances of the particles regarding the nonperiodic dimensions. The final algorithm enables a unified treatment of all types of periodic boundary conditions, for which only the precomputation step has to be adjusted.

Key words and phrases: Ewald summation, nonequispaced fast Fourier transform, particle methods, dipole-dipole interactions, mixed periodicity, NFFT, P2NFFT, P3M

2000 AMS Mathematics Subject Classification: 65T

1 Introduction

For a system of N dipoles at positions $\boldsymbol{x}_j$, located in a box $[-L_1/2, L_1/2] \times [-L_2/2, L_2/2] \times [-L_3/2, L_3/2]$ with dimensions $L_1, L_2, L_3 \in \mathbb{R}_+$, and their dipole moments $\boldsymbol{\mu}_j \in \mathbb{R}^3$ the electrostatic energy is given, in Gaussian units, by

$$
\begin{aligned}
U_{\mathcal{S}} &= \frac{1}{2} \sum_{\boldsymbol{n} \in \mathcal{S}} \sum_{i,j=1}^{N} {}' (\boldsymbol{\mu}_i \cdot \nabla_{\boldsymbol{x}_j})(\boldsymbol{\mu}_i \cdot \nabla_{\boldsymbol{x}_i}) \frac{1}{\|\boldsymbol{x}_{ij} + \boldsymbol{n} \odot \boldsymbol{L}\|} \\
&= \frac{1}{2} \sum_{\boldsymbol{n} \in \mathcal{S}} \sum_{i,j=1}^{N} {}' \frac{\boldsymbol{\mu}_i \cdot \boldsymbol{\mu}_j}{\|\boldsymbol{x}_{ij} + \boldsymbol{n} \odot \boldsymbol{L}\|^3} - \frac{3[\boldsymbol{\mu}_i \cdot (\boldsymbol{x}_{ij} + \boldsymbol{n} \odot \boldsymbol{L})][\boldsymbol{\mu}_j \cdot (\boldsymbol{x}_{ij} + \boldsymbol{n} \odot \boldsymbol{L})]}{\|\boldsymbol{x}_{ij} + \boldsymbol{n} \odot \boldsymbol{L}\|^5},
\end{aligned}
\tag{1.1}
$$

franziska.nestler@mathematik.tu-chemnitz.de
Technische Universität Chemnitz, Faculty of Mathematics, 09107 Chemnitz, Germany

where we use the short notation $\boldsymbol{x}_{ij} := \boldsymbol{x}_i - \boldsymbol{x}_j$ and assume a certain type of periodic boundary conditions, which is specified by the index set $\mathcal{S} \subset \mathbb{Z}^3$. Thereby, we exclude all the terms with $i = j$ in the case $\boldsymbol{n} = \boldsymbol{0}$, which is indicated by the prime on the second sum. By $\odot$ we denote the component wise product, i.e., the translation vectors appearing within the norm are given by

$$\boldsymbol{n} \odot \boldsymbol{L} := (n_1 L_1, n_2 L_2, n_3 L_3) \in \mathbb{R}^3,$$

where $\boldsymbol{n} = (n_1, n_2, n_3) \in \mathbb{Z}^3$ and the edge length vector $\boldsymbol{L}$ is defined by $\boldsymbol{L} := (L_1, L_2, L_3) \in \mathbb{R}^3_+$. The ordinary scalar product is denoted by $\cdot$, i.e., for two vectors $\boldsymbol{y}, \boldsymbol{z} \in \mathbb{R}^3$ we set

$$\boldsymbol{y} \cdot \boldsymbol{z} := y_1 z_1 + y_2 z_2 + y_3 z_3 \in \mathbb{R}.$$

In addition, we are also interested in computing the acting forces, which are for each particle defined via

$$\boldsymbol{F}_{\mathcal{S}}(j) := -\nabla_{\boldsymbol{x}_j} U_{\mathcal{S}}. \tag{1.2}$$

The torque $\boldsymbol{\tau}_{\mathcal{S}}(j) \in \mathbb{R}^3$ acting on the particle j is given by

$$\boldsymbol{\tau}_{\mathcal{S}}(j) := \boldsymbol{\mu}_j \times \boldsymbol{E}_{\mathcal{S}}(j), \tag{1.3}$$

where the vector product is denoted by $\times$ and the electrostatic field $\boldsymbol{E}_{\mathcal{S}}(j) \in \mathbb{R}^3$ is defined via

$$\begin{aligned}
\boldsymbol{E}_{\mathcal{S}}(j) := & -\nabla_{\boldsymbol{\mu}_j} U_{\mathcal{S}} \\
= & -\sum_{\boldsymbol{n} \in \mathcal{S}} \sum_{i=1}^{N}{}' \nabla_{\boldsymbol{x}_j}(\boldsymbol{\mu}_i \cdot \nabla_{\boldsymbol{x}_i}) \frac{1}{\|\boldsymbol{x}_{ij} + \boldsymbol{n} \odot \boldsymbol{L}\|} \\
= & -\sum_{\boldsymbol{n} \in \mathcal{S}} \sum_{i=1}^{N}{}' \frac{\boldsymbol{\mu}_i}{\|\boldsymbol{x}_{ij} + \boldsymbol{n} \odot \boldsymbol{L}\|^3} - \frac{3[\boldsymbol{\mu}_i \cdot (\boldsymbol{x}_{ij} + \boldsymbol{n} \odot \boldsymbol{L})](\boldsymbol{x}_{ij} + \boldsymbol{n} \odot \boldsymbol{L})}{\|\boldsymbol{x}_{ij} + \boldsymbol{n} \odot \boldsymbol{L}\|^5}.
\end{aligned} \tag{1.4}$$

Thus, the energy can also be written as

$$U_{\mathcal{S}} = -\frac{1}{2} \sum_{j=1}^{N} \boldsymbol{\mu}_j \cdot \boldsymbol{E}_{\mathcal{S}}(j). \tag{1.5}$$

If we insert (1.5) into the definition of the forces (1.2) we obtain

$$\boldsymbol{F}_{\mathcal{S}}(j) = \nabla_{\boldsymbol{x}_j} \left[\boldsymbol{\mu}_j \cdot \boldsymbol{E}_{\mathcal{S}}(j) \right]. \tag{1.6}$$

We describe various cases of periodic boundary conditions as follows. Assuming periodic boundary conditions in the first $p \in \{0, 1, 2, 3\}$ dimensions combined with nonperiodic (open) constraints for the remaining $3 - p$ dimensions, we set $\mathcal{S} := \mathbb{Z}^p \times \{0\}^{3-p}$, which effects a replication of the primary box along all dimensions subject to periodic boundary conditions.

Since the summands in (1.1) tend to zero like r^{-3}, where r represents the distance between two particles, the infinite sum is only conditionally convergent for $p = 3$, i.e., an order of summation has to be specified, see [20] for more details. However, also for $p \in \{1, 2\}$ the infinite sum converges very slowly, which makes it impracticable to compute it directly after truncation. For $p = 0$, i.e., no periodic boundary conditions are applied, a direct evaluation is possible within $\mathcal{O}(N^2)$ arithmetic operations, which is not satisfying.

A common approach in the case of periodic boundary conditions is the application of the Ewald summation technique [12], which splits the badly converging sum into two rapidly converging parts in spatial and Fourier domain, respectively. This is explained in Section 1.1 in more detail. In order to compute the Fourier space part efficiently we may apply the FFT. Since the dipoles are not distributed on a uniform mesh, we use the generalization of the FFT to nonequispaced data (nonuniform FFT, NFFT, NUFFT), to which we give a short introduction in Section 1.2. In Section 2 we consider the 3d-periodic case, i.e., $\mathcal{S} := \mathbb{Z}^3$, and show how the electrostatic fields, forces and toques can be approximated based on the Ewald formulas and the NFFT. The same is done in Sections 3–5 for the other types of periodic boundary conditions, respectively. We conclude with a short summary in Section 6.

1.1 Ewald summation

A general approach to compute long range interactions efficiently is the application of the Ewald summation technique [12], which makes use of the simple identity

$$\frac{1}{r} = \frac{\operatorname{erfc}(\alpha r)}{r} + \frac{\operatorname{erf}(\alpha r)}{r}, \tag{1.7}$$

where $\operatorname{erf}(\cdot)$ is the well known error function, $\operatorname{erfc}(\cdot) := 1 - \operatorname{erf}(\cdot)$ is the complementary error function and $\alpha > 0$ is referred to as the splitting parameter. Applying (1.7) the energy (1.1) splits into two parts

$$U_{\mathcal{S}} = \frac{1}{2} \sum_{\boldsymbol{n} \in \mathcal{S}} \sum_{i,j=1}^{N} {}' (\boldsymbol{\mu}_i \cdot \nabla_{\boldsymbol{x}_j})(\boldsymbol{\mu}_i \cdot \nabla_{\boldsymbol{x}_i}) \frac{\operatorname{erfc}(\alpha \|\boldsymbol{x}_{ij} + \boldsymbol{n} \odot \boldsymbol{L}\|)}{\|\boldsymbol{x}_{ij} + \boldsymbol{n} \odot \boldsymbol{L}\|}$$

$$+ \frac{1}{2} \sum_{\boldsymbol{n} \in \mathcal{S}} \sum_{i,j=1}^{N} {}' (\boldsymbol{\mu}_i \cdot \nabla_{\boldsymbol{x}_j})(\boldsymbol{\mu}_i \cdot \nabla_{\boldsymbol{x}_i}) \frac{\operatorname{erf}(\alpha \|\boldsymbol{x}_{ij} + \boldsymbol{n} \odot \boldsymbol{L}\|)}{\|\boldsymbol{x}_{ij} + \boldsymbol{n} \odot \boldsymbol{L}\|},$$

where we refer to

$$U_{\mathcal{S}}^{\text{short}} := \frac{1}{2} \sum_{\boldsymbol{n} \in \mathcal{S}} \sum_{i,j=1}^{N} {}' (\boldsymbol{\mu}_j \cdot \nabla_{\boldsymbol{x}_j})(\boldsymbol{\mu}_i \cdot \nabla_{\boldsymbol{x}_i}) \frac{\operatorname{erfc}(\alpha \|\boldsymbol{x}_{ij} + \boldsymbol{n} \odot \boldsymbol{L}\|)}{\|\boldsymbol{x}_{ij} + \boldsymbol{n} \odot \boldsymbol{L}\|} \tag{1.8}$$

as the short range part. Computing the present derivatives we obtain

$$(\boldsymbol{\mu}_j \cdot \nabla_{\boldsymbol{x}_j})(\boldsymbol{\mu}_i \cdot \nabla_{\boldsymbol{x}_i}) \frac{\operatorname{erfc}(\alpha \|\boldsymbol{x}_{ij} + \boldsymbol{n} \odot \boldsymbol{L}\|)}{\|\boldsymbol{x}_{ij} + \boldsymbol{n} \odot \boldsymbol{L}\|}$$

$$= \left(\frac{2\alpha \mathrm{e}^{-\alpha^2 r^2}}{\sqrt{\pi} r^2} + \frac{\operatorname{erfc}(\alpha r)}{r^3} \right) \left(\boldsymbol{\mu}_j \cdot \boldsymbol{\mu}_i - 3 \frac{(\boldsymbol{\mu}_j \cdot \boldsymbol{r})(\boldsymbol{\mu}_i \cdot \boldsymbol{r})}{r^2} \right) - \frac{4\alpha^3 \mathrm{e}^{-\alpha^2 r^2}}{\sqrt{\pi} r^2} (\boldsymbol{\mu}_j \cdot \boldsymbol{r})(\boldsymbol{\mu}_i \cdot \boldsymbol{r}),$$

where we set $\boldsymbol{r} := \boldsymbol{x}_{ij} + \boldsymbol{n} \odot \boldsymbol{L}$ and $r := \|\boldsymbol{r}\|$. Since the complementary error function $\operatorname{erfc}(r)$ tends to zero exponentially fast in r, the sum (1.8) can be efficiently computed by a direct summation after truncating appropriately.

For the kernel function in the long range part we obtain

$$(\boldsymbol{\mu}_j \cdot \nabla_{\boldsymbol{x}_j})(\boldsymbol{\mu}_i \cdot \nabla_{\boldsymbol{x}_i}) \frac{\operatorname{erf}(\alpha \|\boldsymbol{x}_{ij} + \boldsymbol{n} \odot \boldsymbol{L}\|)}{\|\boldsymbol{x}_{ij} + \boldsymbol{n} \odot \boldsymbol{L}\|}$$

$$= \left(-\frac{2\alpha \mathrm{e}^{-\alpha^2 r^2}}{\sqrt{\pi} r^2} + \frac{\operatorname{erf}(\alpha r)}{r^3} \right) \left(\boldsymbol{\mu}_j \cdot \boldsymbol{\mu}_i - 3 \frac{(\boldsymbol{\mu}_j \cdot \boldsymbol{r})(\boldsymbol{\mu}_i \cdot \boldsymbol{r})}{r^2} \right) + \frac{4\alpha^3 \mathrm{e}^{-\alpha^2 r^2}}{\sqrt{\pi} r^2} (\boldsymbol{\mu}_j \cdot \boldsymbol{r})(\boldsymbol{\mu}_i \cdot \boldsymbol{r}).$$

We compute the limit

$$\lim_{r \to 0} -\frac{2\alpha r e^{-\alpha^2 r^2}}{\sqrt{\pi} r^3} + \frac{\text{erf}(\alpha r)}{r^3} = \frac{4\alpha^3}{3\sqrt{\pi}},$$

and obtain

$$\lim_{\|\boldsymbol{x}_{ij}\| \to 0} (\boldsymbol{\mu}_j \cdot \nabla_{\boldsymbol{x}_j})(\boldsymbol{\mu}_i \cdot \nabla_{\boldsymbol{x}_i}) \frac{\text{erf}(\alpha\|\boldsymbol{x}_{ij}\|)}{\|\boldsymbol{x}_{ij}\|} = \frac{4\alpha^3}{3\sqrt{\pi}} \boldsymbol{\mu}_j \cdot \boldsymbol{\mu}_j = \frac{4\alpha^3}{3\sqrt{\pi}} \|\boldsymbol{\mu}_j\|^2 \qquad (1.9)$$

as well as

$$\frac{1}{2} \sum_{\boldsymbol{n} \in \mathcal{S}} \sum_{i,j=1}^{N} {}' (\boldsymbol{\mu}_i \cdot \nabla_{\boldsymbol{x}_j})(\boldsymbol{\mu}_i \cdot \nabla_{\boldsymbol{x}_i}) \frac{\text{erf}(\alpha\|\boldsymbol{x}_{ij} + \boldsymbol{n} \odot \boldsymbol{L}\|)}{\|\boldsymbol{x}_{ij} + \boldsymbol{n} \odot \boldsymbol{L}\|} = U_{\mathcal{S}}^{\text{long}} + U^{\text{self}}.$$

Thereby, we define the long range part

$$U_{\mathcal{S}}^{\text{long}} := \frac{1}{2} \sum_{\boldsymbol{n} \in \mathcal{S}} \sum_{i,j=1}^{N} (\boldsymbol{\mu}_i \cdot \nabla_{\boldsymbol{x}_j})(\boldsymbol{\mu}_i \cdot \nabla_{\boldsymbol{x}_i}) \frac{\text{erf}(\alpha\|\boldsymbol{x}_{ij} + \boldsymbol{n} \odot \boldsymbol{L}\|)}{\|\boldsymbol{x}_{ij} + \boldsymbol{n} \odot \boldsymbol{L}\|}, \qquad (1.10)$$

where we now insert the finite limit (1.9) in the case $\|\boldsymbol{x}_{ij} + \boldsymbol{n} \odot \boldsymbol{L}\| = 0$, and the self interaction energy

$$U^{\text{self}} := -\frac{2\alpha^3}{3\sqrt{\pi}} \sum_{j=1}^{N} \|\boldsymbol{\mu}_j\|^2, \qquad (1.11)$$

which is the same for all types of periodic boundary conditions. Correspondingly, also the electrostatic fields (1.4), the forces (1.2) as well as the torques (1.3) are split into short ranged and long ranged portions, which we will discuss later in more detail.

The long range part (1.10) is still slowly and in the 3d-periodic case in addition conditionally convergent, but its kernel function does not have a singularity. Thus, this part can be transformed into a sum in Fourier space regarding the periodic dimensions, where in the 3d-periodic case the applied summation order comes into play. We obtain fundamentally different Fourier space representations for the above described types of periodic boundary conditions, see Sections 2–5.

In order to evaluate the obtained Fourier space sum efficiently many methods in the field of molecular dynamics simulations make use of the fast Fourier transform (FFT). Especially for charge-charge (Coulomb) interactions under 3d-periodic constraints a variety of so called particle mesh methods have already been proposed, see [18, 7, 11, 8, 21] and references therein. Since the FFT is a mesh based algorithm, the given continuous charge (or dipole) distribution has at first to be approximated by a grid based charge (dipole) density. This approximation is done by a sum of translates of a so called window function or rather assignment function, which is typically a B-spline. Note that the well known P^3M method has already been generalized to dipolar systems, cf. [6, 5].

The P^2NFFT [27, 28] method, which was also developed for the computation of Coulomb interactions, is based on the FFT for nonequispaced data (NFFT). The NFFT is also a combination of the ordinary FFT and an approximation via a window function and thus the P^2NFFT approach fits very well into the scope of particle mesh methods. Possible window functions are B-splines, but also Gaussians or (Kaiser-)Bessel functions, see [19, 24, 23]. Furthermore, an oversampled FFT can be applied, which makes the tuning of the method

with respect to accuracy as well as efficiency somewhat more flexible, cf. [23]. See [3] for a comparison of the method to other well established algorithms in this field, such as the P³M method, the fast multipole method or multigrid based methods.

Note that we are also able to treat mixed periodic as well as open boundary conditions, see [25, 26]. In contrast to the 3d-periodic case we hereby need a precomputation step, in which the nonperiodic contributions are embed into a periodic setting, such that the NFFT can be applied similarly to the 3d-periodic case. In this paper we show that exactly the same ideas can be applied in the case of dipolar systems.

1.2 The nonequispaced FFT

In the following we give a short overview of the NFFT, see [10, 4, 32, 33, 30, 15, 19], which we start with the introduction of some notations. For some vector $\boldsymbol{M} \in 2\mathbb{N}^d$ we define the index set $\mathcal{I}_{\boldsymbol{M}} \in \mathbb{Z}^d$ by

$$\mathcal{I}_{\boldsymbol{M}} := \bigotimes_{j=1}^{d} \left\{ -\tfrac{M_j}{2}, \ldots, \tfrac{M_j}{2} - 1 \right\}.$$

Furthermore, for $\boldsymbol{x} \in \mathbb{R}^d$ and $\boldsymbol{y} \in \mathbb{R}^d$ (with non vanishing components) we set

$$\boldsymbol{x} \odot \boldsymbol{y} := (x_1 y_1, \ldots, x_d y_d) \in \mathbb{R}^d \quad \text{and} \quad \boldsymbol{x} \oslash \boldsymbol{y} := \left(\tfrac{x_1}{y_1}, \ldots, \tfrac{x_d}{y_d} \right) \in \mathbb{R}^d.$$

For given Fourier coefficients $\hat{f}_{\boldsymbol{k}} \in \mathbb{C}$, $\boldsymbol{k} \in \mathcal{I}_{\boldsymbol{M}}$, consider a trigonometric polynomial

$$f(\boldsymbol{x}) := \sum_{\boldsymbol{k} \in \mathcal{I}_{\boldsymbol{M}}} \hat{f}_{\boldsymbol{k}} e^{-2\pi i \boldsymbol{k} \cdot \boldsymbol{x}},$$

which we aim to evaluate in N given nodes $\boldsymbol{x}_j \in \mathbb{T}^d := \mathbb{R}^d / \mathbb{Z}^d \simeq [-1/2, 1/2)^d$, i.e., we want to compute

$$f_j := f(\boldsymbol{x}_j) = \sum_{\boldsymbol{k} \in \mathcal{I}_{\boldsymbol{M}}} \hat{f}_{\boldsymbol{k}} e^{-2\pi i \boldsymbol{k} \cdot \boldsymbol{x}_j}, \quad j = 1, \ldots, N. \tag{1.12}$$

The straightforward algorithm for the exact computation of (1.12), which is called nonequispaced discrete Fourier transform (NDFT), takes $\mathcal{O}(N|\mathcal{I}_{\boldsymbol{M}}|)$ arithmetic operations. Since we do not have equispaced data we cannot directly apply the FFT in order to evaluate the sums (1.12) more efficiently. The well known NFFT algorithm is a modification of the ordinary FFT and allows an approximate evaluation within $\mathcal{O}(|\mathcal{I}_{\boldsymbol{M}}| \log |\mathcal{I}_{\boldsymbol{M}}| + N)$ arithmetic operations. The basic idea behind the method can be explained as follows.

We approximate f by a sum of equidistant translates of a **1**-periodic window function φ, which should be well localized in spatial as well as in frequency domain. In other words, we approximate f by a discrete convolution of unknown coefficients with a given window function located at points on a uniform grid $\mathcal{I}_{\boldsymbol{m}}$, $\boldsymbol{m} \in 2\mathbb{N}^d$, which reads as

$$f(\boldsymbol{x}) \approx \sum_{\boldsymbol{\ell} \in \mathcal{I}_{\boldsymbol{m}}} g_{\boldsymbol{\ell}} \varphi(\boldsymbol{x} - \boldsymbol{\ell} \oslash \boldsymbol{m}).$$

Thereby, we use the oversampled mesh size $\boldsymbol{m} \geq \boldsymbol{M}$. Applying the aliasing formula and the convolution theorem we obtain

$$\sum_{\boldsymbol{\ell} \in \mathcal{I}_{\boldsymbol{m}}} g_{\boldsymbol{\ell}} \varphi(\boldsymbol{x} - \boldsymbol{\ell} \oslash \boldsymbol{m}) = \sum_{\boldsymbol{k} \in \mathcal{I}_{\boldsymbol{m}}} \sum_{\boldsymbol{r} \in \mathbb{Z}^d} \hat{g}_{\boldsymbol{k}} c_{\boldsymbol{k}+\boldsymbol{r} \odot \boldsymbol{m}}(\varphi) e^{-2\pi i (\boldsymbol{k}+\boldsymbol{r} \odot \boldsymbol{m}) \cdot \boldsymbol{x}}, \tag{1.13}$$

where

$$\hat{g}_{\boldsymbol{k}} := \frac{1}{|\mathcal{I}_{\boldsymbol{m}}|} \sum_{\boldsymbol{\ell} \in \mathcal{I}_{\boldsymbol{m}}} g_{\boldsymbol{\ell}} \, \mathrm{e}^{2\pi\mathrm{i}\boldsymbol{k}\cdot(\boldsymbol{l}\oslash\boldsymbol{m})}, \quad \boldsymbol{k} \in \mathcal{I}_{\boldsymbol{m}},$$

are the discrete Fourier coefficients of $g_{\boldsymbol{\ell}}, \boldsymbol{\ell} \in \mathcal{I}_{\boldsymbol{m}}$, and

$$c_{\boldsymbol{k}}(\varphi) := \int_{\mathbb{T}^d} \varphi(\boldsymbol{x}) \mathrm{e}^{2\pi\mathrm{i}\boldsymbol{k}\cdot\boldsymbol{x}} \mathrm{d}\boldsymbol{x}, \quad \boldsymbol{k} \in \mathbb{Z}^d,$$

are the analytical Fourier coefficients of the window function φ.

We see that it is reasonable so set

$$\hat{g}_{\boldsymbol{k}} := \frac{\hat{f}_{\boldsymbol{k}}}{c_{\boldsymbol{k}}(\varphi)} \ (\boldsymbol{k} \in \mathcal{I}_{\boldsymbol{M}}) \quad \text{and} \quad \hat{g}_{\boldsymbol{k}} := 0 \ (\text{else}), \tag{1.14}$$

since then the Fourier coefficients of the approximation (1.13) coincide with $\hat{f}_{\boldsymbol{k}}$ for all $\boldsymbol{k} \in \mathcal{I}_{\boldsymbol{M}}$ and only the aliasing terms are left. After this step, the coefficients $g_{\boldsymbol{\ell}}$ are obtained by applying the inverse FFT to the coefficients $\hat{g}_{\boldsymbol{k}}$.

Remark 1.1. The approach to set the coefficients $\hat{g}_{\boldsymbol{k}}$ can be further optimized with respect to a specific application. As an example, in the field of particle simulation the root mean square error in the forces is a common measure of accuracy. The optimal coefficients $\hat{g}_{\boldsymbol{k}}$ then depend on which kind of particle interactions are considered (Coulomb, dipolar) as well as which differentiation operator is applied for the computation of the forces. For more details we refer to the derivations of the optimal influence functions for the P^{3}M method, cf. [18, 9] for point charge and [6, 5] for dipolar systems, as well as to [24] for error estimates concerning the P^{2}NFFT method. If the occurrent aliasing terms are left out in the obtained expression for the optimized coefficients $\hat{g}_{\boldsymbol{k}}$, we obtain the standard coefficients (1.14), which we use within the NFFT and the NFFT based particle simulation.

Since the Fourier coefficients in this specific application tend to zero very rapidly, we expect that we can achieve only minor improvements by using an optimized deconvolution approach, see [23] for some numerical examples in the case of Coulomb interactions. $\qquad\square$

The NFFT algorithm can be summarized roughly as follows.

Algorithm 1.1 (NFFT)**.**

Input: nodes $\boldsymbol{x}_j \in \mathbb{T}^d$ ($j = 1, \ldots, N$), coefficients $\hat{f}_{\boldsymbol{k}}$ ($\boldsymbol{k} \in \mathcal{I}_{\boldsymbol{M}}$), oversampled mesh size $\boldsymbol{m} \in 2\mathbb{N}^d$, $\boldsymbol{m} \geq \boldsymbol{M}$.

i) Set $\hat{g}_{\boldsymbol{k}} := \frac{\hat{f}_{\boldsymbol{k}}}{c_{\boldsymbol{k}}(\varphi)}$ for all $\boldsymbol{k} \in \mathcal{I}_{\boldsymbol{M}}$ and $\hat{g}_{\boldsymbol{k}} := 0$ for $\boldsymbol{k} \in \mathcal{I}_{\boldsymbol{m}} \setminus \mathcal{I}_{\boldsymbol{M}}$.

Complexity: $\mathcal{O}(|\mathcal{I}_{\boldsymbol{M}}|)$.

ii) Use the inverse FFT for the computation of the coefficients

$$g_l = \frac{1}{|\mathcal{I}_{\boldsymbol{m}}|} \sum_{\boldsymbol{k} \in \mathcal{I}_{\boldsymbol{m}}} \hat{g}_{\boldsymbol{k}} \, \mathrm{e}^{-2\pi\mathrm{i}\boldsymbol{k}\cdot(\boldsymbol{l}\oslash\boldsymbol{m})}, \quad \boldsymbol{l} \in \mathcal{I}_{\boldsymbol{m}}.$$

Complexity: $\mathcal{O}(|\mathcal{I}_{\boldsymbol{m}}| \log |\mathcal{I}_{\boldsymbol{m}}|)$.

iii) Compute
$$f(\boldsymbol{x}_j) \approx f_{\approx}(\boldsymbol{x}_j) := \sum_{l \in \mathcal{I}_{\boldsymbol{m}}} g_l \varphi\left(\boldsymbol{x}_j - \boldsymbol{l} \oslash \boldsymbol{m}\right)$$

for all $j = 1, \ldots, N$. The sums are short due to the good localization or rather small support of the window function φ. Complexity: $\mathcal{O}(N)$.

Output: Approximate function values $f_{\approx}(\boldsymbol{x}_j) \approx f(\boldsymbol{x}_j)$ for all $j = 1, \ldots, N$. □

The computation of sums of the form

$$h(\boldsymbol{k}) := \sum_{j=1}^{N} f_j \mathrm{e}^{2\pi \mathrm{i} \boldsymbol{k} \cdot \boldsymbol{x}_j}, \quad \boldsymbol{k} \in \mathcal{I}_{\boldsymbol{M}}, \tag{1.15}$$

where now the coefficients f_j are given, is a very similar problem. Considering (1.12) as the computation of a matrix vector product, the matrix representing (1.15) is obtained by adjoining the matrix from (1.12). Thus, the efficient algorithm is known as the adjoint NFFT and can be summarized as follows.

Algorithm 1.2 (adjoint NFFT).

Input: nodes $\boldsymbol{x}_j$ and corresponding coefficients f_j, $j = 1, \ldots, N$, mesh size $\boldsymbol{M} \in 2\mathbb{N}^d$ and oversampled mesh size $\boldsymbol{m} \in 2\mathbb{N}^d$, $\boldsymbol{m} \geq \boldsymbol{M}$.

i) Set
$$g_{\boldsymbol{\ell}} := \sum_{j=1}^{N} f_j \varphi\left(\boldsymbol{x}_j - \boldsymbol{l} \oslash \boldsymbol{m}\right)$$

for all $\boldsymbol{\ell} \in \mathcal{I}_{\boldsymbol{m}}$. The sums are short due to the good localization or rather small support of the window function φ. Complexity: $\mathcal{O}(N)$.

ii) Use the FFT for the computation of the coefficients

$$\hat{g}_{\boldsymbol{k}} = \frac{1}{|\mathcal{I}_{\boldsymbol{m}}|} \sum_{\boldsymbol{\ell} \in \mathcal{I}_{\boldsymbol{m}}} g_{\boldsymbol{\ell}} \, \mathrm{e}^{2\pi \mathrm{i} \boldsymbol{k} \cdot (\boldsymbol{l} \oslash \boldsymbol{m})}, \quad \boldsymbol{k} \in \mathcal{I}_{\boldsymbol{m}}.$$

Complexity: $\mathcal{O}(|\mathcal{I}_{\boldsymbol{m}}| \log |\mathcal{I}_{\boldsymbol{m}}|)$.

iii) Set $h(\boldsymbol{k}) \approx h_{\approx}(\boldsymbol{k}) := \frac{\hat{g}_{\boldsymbol{k}}}{c_{\boldsymbol{k}}(\varphi)}$ for all $\boldsymbol{k} \in \mathcal{I}_{\boldsymbol{M}}$. Complexity: $\mathcal{O}(|\mathcal{I}_{\boldsymbol{M}}|)$.

Output: Approximations $h_{\approx}(\boldsymbol{k}) \approx h(\boldsymbol{k})$ for all $\boldsymbol{k} \in \mathcal{I}_{\boldsymbol{M}}$. □

2 Periodic boundary conditions in all three dimensions

We are now interested in the fast computation of dipole-dipole interactions subject to fully periodic boundary conditions. We define the resulting energy via

$$U^{\mathrm{3d}} := U_{\mathbb{Z}^3},$$

i.e., we set $\mathcal{S} = \mathbb{Z}^3$ in (1.1). As derived in the introduction we can write

$$U^{\mathrm{3d}} = U^{\mathrm{3d,short}} + U^{\mathrm{3d,long}} + U^{\mathrm{self}},$$

where we set

$$U^{\text{3d,short}} := U_{\mathbb{Z}^3}^{\text{short}} = \frac{1}{2} \sum_{\boldsymbol{n} \in \mathbb{Z}^3} \sum_{i,j=1}^{N} {}' (\boldsymbol{\mu}_j \cdot \nabla_{\boldsymbol{x}_j})(\boldsymbol{\mu}_i \cdot \nabla_{\boldsymbol{x}_i}) \frac{\text{erfc}(\alpha \|\boldsymbol{x}_{ij} + \boldsymbol{n} \odot \boldsymbol{L}\|)}{\|\boldsymbol{x}_{ij} + \boldsymbol{n} \odot \boldsymbol{L}\|}, \tag{2.1}$$

$$U^{\text{3d,long}} := U_{\mathbb{Z}^3}^{\text{long}} = \frac{1}{2} \sum_{\boldsymbol{n} \in \mathbb{Z}^3} \sum_{i,j=1}^{N} (\boldsymbol{\mu}_j \cdot \nabla_{\boldsymbol{x}_j})(\boldsymbol{\mu}_i \cdot \nabla_{\boldsymbol{x}_i}) \frac{\text{erf}(\alpha \|\boldsymbol{x}_{ij} + \boldsymbol{n} \odot \boldsymbol{L}\|)}{\|\boldsymbol{x}_{ij} + \boldsymbol{n} \odot \boldsymbol{L}\|},$$

and the self interaction energy U^{self} is defined in (1.11).

The transformation of $U^{\text{3d,long}}$ into Fourier space under the assumption of a spherical summation order gives, see [20, Section 4],

$$U^{\text{3d,long}} = U^{\text{3d,F}} + U^{\text{3d,0}},$$

where we define the Fourier sum

$$U^{\text{3d,F}} := \frac{1}{2\pi V} \sum_{\boldsymbol{k} \in \mathbb{Z}^3} \hat{\psi}(\boldsymbol{k}) \sum_{i,j=1}^{N} (\boldsymbol{\mu}_i \cdot \nabla_{\boldsymbol{x}_i})(\boldsymbol{\mu}_j \cdot \nabla_{\boldsymbol{x}_j}) e^{2\pi i (\boldsymbol{k} \oslash \boldsymbol{L}) \cdot \boldsymbol{x}_{ij}} \tag{2.2}$$

$$= \frac{1}{2\pi V} \sum_{\boldsymbol{k} \in \mathbb{Z}^3} \hat{\psi}(\boldsymbol{k}) \left| \sum_{i=1}^{N} (\boldsymbol{\mu}_i \cdot \nabla_{\boldsymbol{x}_i}) e^{2\pi i (\boldsymbol{k} \oslash \boldsymbol{L}) \cdot \boldsymbol{x}_i} \right|^2$$

$$= \frac{2\pi}{V} \sum_{\boldsymbol{k} \in \mathbb{Z}^3} \hat{\psi}(\boldsymbol{k}) \left| (\boldsymbol{k} \oslash \boldsymbol{L}) \cdot \sum_{i=1}^{N} \boldsymbol{\mu}_i e^{2\pi i (\boldsymbol{k} \oslash \boldsymbol{L}) \cdot \boldsymbol{x}_i} \right|^2$$

with the Fourier coefficients

$$\hat{\psi}(\boldsymbol{k}) := \begin{cases} \dfrac{e^{-\pi^2 \|\boldsymbol{k} \oslash \boldsymbol{L}\|^2 / \alpha^2}}{\|\boldsymbol{k} \oslash \boldsymbol{L}\|^2} & : \boldsymbol{k} \neq \boldsymbol{0}, \\ 0 & : \boldsymbol{k} = \boldsymbol{0}, \end{cases}$$

and the $\boldsymbol{k} = \boldsymbol{0}$ contribution, also known as the surface term, by

$$U^{\text{3d,0}} := \frac{2\pi}{3V} \sum_{i=1}^{N} \sum_{j=1}^{N} \boldsymbol{\mu}_i \cdot \boldsymbol{\mu}_j = \frac{2\pi}{3V} \left\| \sum_{i=1}^{N} \boldsymbol{\mu}_i \right\|^2. \tag{2.3}$$

Thereby we denote by $V := L_1 L_2 L_3$ the volume of the Box.

Remark 2.1. The surface term $U^{\text{3d,0}}$ is the only part, which depends on the applied summation order. In the literature, see for instance [14, page 304], one often finds

$$U^{\text{3d,0}} := \frac{2\pi}{(2\epsilon' + 1)V} \sum_{i=1}^{N} \sum_{j=1}^{N} \boldsymbol{\mu}_i \cdot \boldsymbol{\mu}_j,$$

where ϵ' is the dielectric constant of the surrounding medium. For vacuum we have $\varepsilon' = 1$ and (2.3) applies. If metallic boundary conditions are applied, we have $\epsilon' = \infty$ and the surface term vanishes.

In the case of Coulomb interactions we have

$$U^{3\mathrm{d},\mathrm{F}} = \frac{1}{2\pi V} \sum_{\boldsymbol{k}\in\mathbb{Z}^3} \hat{\psi}(\boldsymbol{k}) \left| \sum_{i=1}^{N} q_i \mathrm{e}^{2\pi\mathrm{i}(\boldsymbol{k}\oslash\boldsymbol{L})\cdot\boldsymbol{x}_i} \right|^2,$$

$$U^{3\mathrm{d},0} = \frac{2\pi}{3V} \sum_{i=1}^{N} \sum_{i=1}^{N} q_i q_j (\boldsymbol{x}_i \cdot \boldsymbol{x}_j) = \frac{2\pi}{3V} \left\| \sum_{i=1}^{N} q_i \boldsymbol{x}_i \right\|^2,$$

which can be obtained by using convergence factors, see [20]. Obviously, we simply have to replace the charges q_i by the operators $\boldsymbol{\mu}_i \cdot \nabla_{\boldsymbol{x}_i}$ to obtain (2.2) and (2.3), which are valid for dipole-dipole interactions. $\qquad\square$

2.1 Computation of the electrostatic fields and torques

Based on the decomposition of the energy

$$U^{3\mathrm{d}} = U^{3\mathrm{d},\mathrm{short}} + U^{3\mathrm{d},\mathrm{F}} + U^{3\mathrm{d},0} + U^{\mathrm{self}},$$

the electrostatic fields of the single dipoles, which we define via (1.4), can be written as

$$\boldsymbol{E}^{3\mathrm{d}}(j) := \boldsymbol{E}_{\mathbb{Z}^3}(j) = \boldsymbol{E}^{3\mathrm{d},\mathrm{short}}(j) + \boldsymbol{E}^{3\mathrm{d},\mathrm{F}}(j) + \boldsymbol{E}^{3\mathrm{d},0}(j) + \boldsymbol{E}^{\mathrm{self}}(j).$$

Thereby, we define the short range part

$$\boldsymbol{E}^{3\mathrm{d},\mathrm{short}}(j) := \boldsymbol{E}^{\mathrm{short}}_{\mathbb{Z}^3}(j),$$

where we define for $\mathcal{S} \subset \mathbb{Z}^3$

$$\boldsymbol{E}^{\mathrm{short}}_{\mathcal{S}}(j) := -\nabla_{\boldsymbol{x}_j} \sum_{\boldsymbol{n}\in\mathcal{S}} \sum_{i=1}^{N}{}' (\boldsymbol{\mu}_i \cdot \nabla_{\boldsymbol{x}_i}) \frac{\mathrm{erfc}(\alpha\|\boldsymbol{x}_{ij} + \boldsymbol{n}\odot\boldsymbol{L}\|)}{\|\boldsymbol{x}_{ij} + \boldsymbol{n}\odot\boldsymbol{L}\|}. \tag{2.4}$$

Furthermore, we have

$$\boldsymbol{E}^{3\mathrm{d},\mathrm{F}}(j) = -\frac{\nabla_{\boldsymbol{x}_j}}{\pi V} \sum_{\boldsymbol{k}\in\mathbb{Z}^3} \hat{\psi}(\boldsymbol{k}) \left(\sum_{i=1}^{N} (\boldsymbol{\mu}_i \cdot \nabla_{\boldsymbol{x}_i}) \mathrm{e}^{2\pi\mathrm{i}(\boldsymbol{k}\oslash\boldsymbol{L})\cdot\boldsymbol{x}_i} \right) \mathrm{e}^{-2\pi\mathrm{i}(\boldsymbol{k}\oslash\boldsymbol{L})\cdot\boldsymbol{x}_j} \tag{2.5}$$

$$= -\frac{4\pi}{V} \sum_{\boldsymbol{k}\in\mathbb{Z}^3} \hat{\psi}(\boldsymbol{k})(\boldsymbol{k}\oslash\boldsymbol{L}) \left[(\boldsymbol{k}\oslash\boldsymbol{L}) \cdot \boldsymbol{S}(\boldsymbol{k}) \right] \mathrm{e}^{-2\pi\mathrm{i}(\boldsymbol{k}\oslash\boldsymbol{L})\cdot\boldsymbol{x}_j} \tag{2.6}$$

with the structure factors

$$\boldsymbol{S}(\boldsymbol{k}) = \sum_{i=1}^{N} \boldsymbol{\mu}_i \mathrm{e}^{2\pi\mathrm{i}(\boldsymbol{k}\oslash\boldsymbol{L})\cdot\boldsymbol{x}_i}, \tag{2.7}$$

and

$$\boldsymbol{E}^{3\mathrm{d},0}(j) = -\frac{4\pi}{3V} \sum_{i=1}^{N} \boldsymbol{\mu}_i,$$

$$\boldsymbol{E}^{\mathrm{self}}(j) = \frac{4\alpha^3}{3\sqrt{\pi}} \boldsymbol{\mu}_j. \tag{2.8}$$

These identities follow immediately from the Ewald formulas (2.1), (2.2), (2.3) and (1.11) for the energy U^{3d}, since the energy is simply a sum over the scalar products $\boldsymbol{\mu}_i \cdot \boldsymbol{E}^{\mathrm{3d}}(i)$, see equation (1.5).

As already pointed out, the short range parts $\boldsymbol{E}^{\mathrm{3d,short}}(j)$ can be obtained by a direct evaluation, i.e., we can compute an approximation $\boldsymbol{E}_{\approx}^{\mathrm{3d,short}}(j)$ via (2.4) by just considering distances $\|\boldsymbol{x}_{ij} + \boldsymbol{n} \odot \boldsymbol{L}\| \leq r_{\mathrm{cut}}$, where $r_{\mathrm{cut}} > 0$ is an appropriate cutoff radius. Further, the computation of $\boldsymbol{E}^{\mathrm{3d,0}}(j)$ as well as $\boldsymbol{E}^{\mathrm{self}}(j)$ for all $j = 1, \ldots, N$ is straight forward and only takes $\mathcal{O}(N)$ arithmetic operations. The efficient approximation of the Fourier space contributions $\boldsymbol{E}^{\mathrm{3d,F}}(j)$, $j = 1, \ldots, N$, can be realized as follows.

The first approach is based on (2.6), i.e., the differentiation is done in Fourier space. We refer to this as the i$\boldsymbol{k}$-differentiation approach.

Algorithm 2.1 (Approximate $\boldsymbol{E}^{\mathrm{3d,F}}(j)$, i$\boldsymbol{k}$-differentiation)**.**

Input: positions $\boldsymbol{x}_j \in \bigotimes_{i=1}^3 [-L_i/2, L_i/2]$ and corresponding dipole moments $\boldsymbol{\mu}_j \in \mathbb{R}^3$ ($j = 1, \ldots, N$), splitting parameter $\alpha > 0$, far field cutoff $\boldsymbol{M} \in 2\mathbb{N}^3$, NFFT parameters (window function, oversampling).

   i) Approximate the structure factors $\boldsymbol{S}(\boldsymbol{k}) \approx \boldsymbol{S}_{\approx}(\boldsymbol{k})$, $\boldsymbol{k} \in \mathcal{I}_{\boldsymbol{M}}$, as defined in (2.7), by an adjoint NFFT in each component (three adjoint 3d-NFFTs).

  ii) Compute the scalar products $(\boldsymbol{k} \oslash \boldsymbol{L}) \cdot \boldsymbol{S}_{\approx}(\boldsymbol{k})$ for all $\boldsymbol{k} \in \mathcal{I}_{\boldsymbol{M}}$.

 iii) Approximate the Fourier sums

$$-\frac{4\pi}{V} \sum_{\boldsymbol{k} \in \mathcal{I}_{\boldsymbol{M}}} \hat{\psi}(\boldsymbol{k})(\boldsymbol{k} \oslash \boldsymbol{L}) \left[(\boldsymbol{k} \oslash \boldsymbol{L}) \cdot \boldsymbol{S}_{\approx}(\boldsymbol{k}) \right] \mathrm{e}^{-2\pi \mathrm{i}(\boldsymbol{k} \oslash \boldsymbol{L}) \cdot \boldsymbol{x}_j} \stackrel{\mathrm{NFFT}}{\approx} \boldsymbol{E}_{\approx}^{\mathrm{3d,F}}(j)$$

     by applying an NFFT in each component (three 3d-NFFTs).

Output: approximate Fourier space parts of the fields $\boldsymbol{E}_{\approx}^{\mathrm{3d,F}}(j) \approx \boldsymbol{E}^{\mathrm{3d,F}}(j)$, $j = 1, \ldots, N$.   □

A second approach follows (2.5) and applies the differentiation operator to the NFFT window function φ. We refer to this method as the analytical differentiation approach.

Algorithm 2.2 (Approximate $\boldsymbol{E}^{\mathrm{3d,F}}(j)$, analytic differentiation)**.**

Input: positions $\boldsymbol{x}_j \in \bigotimes_{i=1}^3 [-L_i/2, L_i/2]$ and corresponding dipole moments $\boldsymbol{\mu}_j \in \mathbb{R}^3$ ($j = 1, \ldots, N$), splitting parameter $\alpha > 0$, far field cutoff $\boldsymbol{M} \in 2\mathbb{N}^3$, NFFT parameters (window function, oversampling).

   i) Use the adjoint NFFT to approximate for all $\boldsymbol{k} \in \mathcal{I}_{\boldsymbol{M}}$ the sums

$$A(\boldsymbol{k}) := \sum_{i=1}^N (\boldsymbol{\mu}_i \cdot \nabla_{\boldsymbol{x}_i}) \mathrm{e}^{2\pi \mathrm{i}(\boldsymbol{k} \oslash \boldsymbol{L}) \cdot \boldsymbol{x}_i} \stackrel{\mathrm{NFFT^H}}{\approx} A_{\approx}(\boldsymbol{k}), \tag{2.9}$$

    i.e, we replace step 1 of Algorithm 1.2 by

$$g_{\boldsymbol{\ell}} := \sum_{i=1}^N (\boldsymbol{\mu}_i \oslash \boldsymbol{L}) \cdot \nabla \varphi(\boldsymbol{x}_i \oslash \boldsymbol{L} - \boldsymbol{\ell} \oslash \boldsymbol{m}).$$

    This means that we only need to compute one 3d-FFT (see step 2 in Algorithm 1.2), while spending more effort in step 1.

ii) Approximate the Fourier space parts of the fields

$$-\frac{\nabla_{\boldsymbol{x}_j}}{\pi V} \sum_{\boldsymbol{k} \in \mathcal{I}_{\boldsymbol{M}}} \hat{\psi}(\boldsymbol{k}) A_{\approx}(\boldsymbol{k}) \mathrm{e}^{-2\pi \mathrm{i}(\boldsymbol{k} \oslash \boldsymbol{L}) \cdot \boldsymbol{x}_j} \overset{\mathrm{NFFT}}{\approx} \boldsymbol{E}_{\approx}^{3\mathrm{d},\mathrm{F}}(j)$$

by applying the NFFT, i.e., set $\hat{f}_{\boldsymbol{k}} := -\frac{1}{\pi V}\hat{\psi}(\boldsymbol{k}) A_{\approx}(\boldsymbol{k})$ in Algorithm 1.1 and replace step 3 by

$$\boldsymbol{E}_{\approx}^{3\mathrm{d},\mathrm{F}}(j) := \left(\sum_{\boldsymbol{\ell} \in \mathcal{I}_{\boldsymbol{m}}} g_{\boldsymbol{\ell}} \nabla \varphi(\boldsymbol{x}_j \oslash \boldsymbol{L} - \boldsymbol{\ell} \oslash \boldsymbol{m}) \right) \oslash \boldsymbol{L}.$$

Again, we only need to compute one inverse 3d-FFT (see step 2 in Algorithm 1.1), but step 3 is somewhat more expensive. The computed vectors have to be divided by $\boldsymbol{L}$ (component wise), which follows immediately from the chain rule.

Output: approximate Fourier space parts of the fields $\boldsymbol{E}_{\approx}^{3\mathrm{d},\mathrm{F}}(j) \approx \boldsymbol{E}^{3\mathrm{d},\mathrm{F}}(j)$, $j = 1, \ldots, N$. □

Note that the above described approach is very similar to the P^{3}M method for dipolar interactions if the NFFT is applied without oversampling and with a B-spline as window function φ. See [6] for a description of the P^{3}M method based on the i$\boldsymbol{k}$-differentiation approach and error estimates as well as [5] for the analytical differentiation approach, corresponding error estimates and some comparisons between the two different differentiation schemes.

Based on the computed approximations of the fields

$$\boldsymbol{E}_{\approx}^{3\mathrm{d}}(j) := \boldsymbol{E}_{\approx}^{3\mathrm{d},\mathrm{short}}(j) + \boldsymbol{E}_{\approx}^{3\mathrm{d},\mathrm{F}}(j) + \boldsymbol{E}^{3\mathrm{d},0}(j) + \boldsymbol{E}^{\mathrm{self}}(j)$$

the torques are simply obtained by (1.3), i.e., we approximate the torques by

$$\boldsymbol{\tau}^{3\mathrm{d}}(j) \approx \boldsymbol{\tau}_{\approx}^{3\mathrm{d}}(j) := \boldsymbol{\mu}_j \times \boldsymbol{E}_{\approx}^{3\mathrm{d}}(j).$$

Following the identity (1.5), an approximation of the energy $U^{3\mathrm{d}}$ is given by

$$U_{\approx}^{3\mathrm{d}} := -\frac{1}{2} \sum_{j=1}^{N} \boldsymbol{\mu}_j \cdot \boldsymbol{E}_{\approx}^{3\mathrm{d}}(j).$$

2.2 Computation of the forces

The forces are obtained by applying (1.6). Since the contributions $\boldsymbol{E}^{3\mathrm{d},0}(j)$ and $\boldsymbol{E}^{3\mathrm{d},\mathrm{self}}(j)$ do not depend on the particle positions, we obtain with (1.6) and the Ewald summation formulas for the fields $\boldsymbol{E}^{3\mathrm{d}}(j)$

$$\boldsymbol{F}^{3\mathrm{d}}(j) = \nabla_{\boldsymbol{x}_j} \left[\boldsymbol{\mu}_j \cdot \boldsymbol{E}^{3\mathrm{d}}(j) \right] = \boldsymbol{F}^{3\mathrm{d},\mathrm{short}}(j) + \boldsymbol{F}^{3\mathrm{d},\mathrm{F}}(j),$$

where we define the short range parts by

$$\boldsymbol{F}_{\mathcal{S}}^{\mathrm{short}}(j) := -\nabla_{\boldsymbol{x}_j}(\boldsymbol{\mu}_j \cdot \nabla_{\boldsymbol{x}_j}) \sum_{\boldsymbol{n} \in \mathcal{S}} \sum_{i=1}^{N}{}'(\boldsymbol{\mu}_i \cdot \nabla_{\boldsymbol{x}_i}) \frac{\mathrm{erfc}(\alpha \|\boldsymbol{x}_{ij} + \boldsymbol{n} \odot \boldsymbol{L}\|)}{\|\boldsymbol{x}_{ij} + \boldsymbol{n} \odot \boldsymbol{L}\|} \qquad (2.10)$$

and set $\boldsymbol{F}^{3\mathrm{d},\mathrm{short}}(j) := \boldsymbol{F}_{\mathbb{Z}^3}^{\mathrm{short}}(j)$. We can compute an approximation $\boldsymbol{F}_{\approx}^{3\mathrm{d},\mathrm{short}}(j)$ for each j by simply truncating the sum (2.10), i.e., for an appropriate cutoff radius r_{cut} we only consider distances $\|\boldsymbol{x}_{ij} + \boldsymbol{n} \odot \boldsymbol{L}\| \leq r_{\mathrm{cut}}$.

Again, we may apply the i$\boldsymbol{k}$-differentiation or the analytical differentiation approach. If the differentiation operators are applied in Fourier space we obtain from (2.5) and (2.6)

$$
\begin{aligned}
\boldsymbol{F}^{3\mathrm{d,F}}(j) &:= \nabla_{\boldsymbol{x}_j} \left[\boldsymbol{\mu}_j \cdot \boldsymbol{E}^{3\mathrm{d,F}}(j) \right] \\
&= -\frac{\nabla_{\boldsymbol{x}_j}}{\pi V} (\boldsymbol{\mu}_j \cdot \nabla_{\boldsymbol{x}_j}) \sum_{\boldsymbol{k} \in \mathbb{Z}^3} \hat{\psi}(\boldsymbol{k}) \left(\sum_{i=1}^{N} (\boldsymbol{\mu}_i \cdot \nabla_{\boldsymbol{x}_i}) \mathrm{e}^{2\pi\mathrm{i}(\boldsymbol{k}\oslash\boldsymbol{L})\cdot\boldsymbol{x}_i} \right) \mathrm{e}^{-2\pi\mathrm{i}(\boldsymbol{k}\oslash\boldsymbol{L})\cdot\boldsymbol{x}_j} \quad (2.11) \\
&= \frac{8\pi^2\mathrm{i}}{V} \sum_{\boldsymbol{k} \in \mathbb{Z}^3} \hat{\psi}(\boldsymbol{k}) \left[\boldsymbol{\mu}_j \cdot (\boldsymbol{k} \oslash \boldsymbol{L}) \right] \left[(\boldsymbol{k} \oslash \boldsymbol{L}) \cdot \boldsymbol{S}(\boldsymbol{k}) \right] (\boldsymbol{k} \oslash \boldsymbol{L}) \, \mathrm{e}^{-2\pi\mathrm{i}(\boldsymbol{k}\oslash\boldsymbol{L})\cdot\boldsymbol{x}_j} \\
&= \frac{8\pi^2\mathrm{i}}{V} \left(\sum_{\boldsymbol{k} \in \mathbb{Z}^3} \hat{\psi}(\boldsymbol{k})(\boldsymbol{k} \oslash \boldsymbol{L})(\boldsymbol{k} \oslash \boldsymbol{L})^\top \left[(\boldsymbol{k} \oslash \boldsymbol{L}) \cdot \boldsymbol{S}(\boldsymbol{k}) \right] \mathrm{e}^{-2\pi\mathrm{i}(\boldsymbol{k}\oslash\boldsymbol{L})\cdot\boldsymbol{x}_j} \right) \boldsymbol{\mu}_j,
\end{aligned}
$$

i.e., in order to approximate the outer sums we have to compute a 3d-FFT in all 9 components. Applying symmetry properties, we can reduce the amount of work to the computation of 6 FFTs in three variables.

Algorithm 2.3 (Approximate $\boldsymbol{F}^{3\mathrm{d,F}}(j)$, i$\boldsymbol{k}$-differentiation)**.**

Input: positions $\boldsymbol{x}_j \in \bigotimes_{i=1}^{3}[-L_i/2, L_i/2]$ and corresponding dipole moments $\boldsymbol{\mu}_j \in \mathbb{R}^3$ ($j = 1, \ldots, N$), splitting parameter $\alpha > 0$, far field cutoff $\boldsymbol{M} \in 2\mathbb{N}^3$, NFFT parameters (window function, oversampling).

i) Approximate the structure factors $\boldsymbol{S}(\boldsymbol{k}) \approx \boldsymbol{S}_{\approx}(\boldsymbol{k})$, $\boldsymbol{k} \in \mathcal{I}_{\boldsymbol{M}}$, as defined in (2.7), by an adjoint NFFT in each component (three adjoint 3d-NFFTs).

ii) Compute the scalar products $(\boldsymbol{k} \oslash \boldsymbol{L}) \cdot \boldsymbol{S}_{\approx}(\boldsymbol{k})$ for all $\boldsymbol{k} \in \mathcal{I}_{\boldsymbol{M}}$.

iii) Approximate the matrix-valued sums

$$
\frac{8\pi^2\mathrm{i}}{V} \sum_{\boldsymbol{k} \in \mathcal{I}_{\boldsymbol{M}}} \hat{\psi}(\boldsymbol{k})(\boldsymbol{k} \oslash \boldsymbol{L})(\boldsymbol{k} \oslash \boldsymbol{L})^\top \left[(\boldsymbol{k} \oslash \boldsymbol{L}) \cdot \boldsymbol{S}_{\approx}(\boldsymbol{k}) \right] \mathrm{e}^{-2\pi\mathrm{i}(\boldsymbol{k}\oslash\boldsymbol{L})\cdot\boldsymbol{x}_j} \stackrel{\mathrm{NFFT}}{\approx} \boldsymbol{T}(j)
$$

by applying an NFFT in each component (six 3d-NFFTs, exploit symmetry properties).

iv) Finally, the Fourier space parts of the forces are approximated by computing the matrix-vector products

$$
\boldsymbol{F}^{3\mathrm{d,F}}_{\approx}(j) := \boldsymbol{T}(j)\boldsymbol{\mu}_j.
$$

Output: approximate Fourier space parts of the forces $\boldsymbol{F}^{3\mathrm{d,F}}_{\approx}(j) \approx \boldsymbol{F}^{3\mathrm{d,F}}(j)$, $j = 1, \ldots, N$. □

For the analytical differentiation approach we write the Fourier space contributions of the forces based on (2.11) as

$$
\begin{aligned}
\boldsymbol{F}^{3\mathrm{d,F}}(j) &= -\frac{\nabla_{\boldsymbol{x}_j}}{\pi V} (\boldsymbol{\mu}_j \cdot \nabla_{\boldsymbol{x}_j}) \sum_{\boldsymbol{k} \in \mathcal{I}_{\boldsymbol{M}}} \hat{\psi}(\boldsymbol{k}) A(\boldsymbol{k}) \, \mathrm{e}^{-2\pi\mathrm{i}(\boldsymbol{k}\oslash\boldsymbol{L})\cdot\boldsymbol{x}_j} \\
&= -\frac{1}{\pi V} (\nabla_{\boldsymbol{x}_j} \nabla_{\boldsymbol{x}_j}^\top) \boldsymbol{\mu}_j \sum_{\boldsymbol{k} \in \mathcal{I}_{\boldsymbol{M}}} \hat{\psi}(\boldsymbol{k}) A(\boldsymbol{k}) \, \mathrm{e}^{-2\pi\mathrm{i}(\boldsymbol{k}\oslash\boldsymbol{L})\cdot\boldsymbol{x}_j},
\end{aligned}
$$

where we define the sums $A(\boldsymbol{k})$ in (2.9) and the operator $\nabla_{\boldsymbol{x}_j} \nabla_{\boldsymbol{x}_j}^\top$ symbolizes the application of the Hessian matrix.

Algorithm 2.4 (Approximate $\boldsymbol{F}^{\mathrm{3d,F}}(j)$, analytic differentiation)**.**

Input: positions $\boldsymbol{x}_j \in \bigotimes_{i=1}^{3}[-L_i/2, L_i/2]$ and corresponding dipole moments $\boldsymbol{\mu}_j \in \mathbb{R}^3$ ($j = 1, \ldots, N$), splitting parameter $\alpha > 0$, far field cutoff $\boldsymbol{M} \in 2\mathbb{N}^3$, NFFT parameters (window function, oversampling).

i) Use the adjoint NFFT to approximate the sums $A(\boldsymbol{k}) \approx A_\approx(\boldsymbol{k})$, $\boldsymbol{k} \in \mathcal{I}_{\boldsymbol{M}}$, as defined in (2.9), i.e, we replace step 1 of Algorithm 1.2 by

$$g_{\boldsymbol{\ell}} := \sum_{i=1}^{N} (\boldsymbol{\mu}_i \oslash \boldsymbol{L}) \cdot \nabla\varphi(\boldsymbol{x}_i \oslash \boldsymbol{L} - \boldsymbol{\ell} \oslash \boldsymbol{m}).$$

This means that we only need to compute one 3d-FFT (see step 2 of Algorithm 1.2), whereas step 1 is now more expensive.

ii) Apply the NFFT to approximate the sums

$$-\frac{1}{\pi V}(\nabla_{\boldsymbol{x}_j} \nabla_{\boldsymbol{x}_j}^{\top}) \sum_{\boldsymbol{k} \in \mathcal{I}_{\boldsymbol{M}}} \hat{\psi}(\boldsymbol{k}) A_\approx(\boldsymbol{k}) \mathrm{e}^{-2\pi\mathrm{i}(\boldsymbol{k} \oslash \boldsymbol{L}) \cdot \boldsymbol{x}_j} \overset{\mathrm{NFFT}}{\approx} \boldsymbol{T}(j),$$

i.e., set $\hat{f}_{\boldsymbol{k}} := -\frac{1}{\pi V}\hat{\psi}(\boldsymbol{k}) A_\approx(\boldsymbol{k})$ in Algorithm 1.1 and replace step 3 by

$$\boldsymbol{T}(j) := \sum_{\boldsymbol{\ell} \in \mathcal{I}_{\boldsymbol{m}}} g_{\boldsymbol{\ell}} \, \mathbf{H}(\varphi)(\boldsymbol{x}_j \oslash \boldsymbol{L} - \boldsymbol{\ell} \oslash \boldsymbol{m}),$$

where we denote by $\mathbf{H}(\varphi)(\cdot)$ the Hessian matrix of the window function φ. Again, we only need to compute one inverse 3d-FFT (see step 2 in Algorithm 1.12), whereas step 3 is now more expensive.

iii) Finally, the Fourier space parts of the forces are approximated by computing the matrix-vector products

$$\boldsymbol{F}_\approx^{\mathrm{3d,F}}(j) := \mathrm{diag}(\boldsymbol{L})^{-1}\boldsymbol{T}(j)\mathrm{diag}(\boldsymbol{L})^{-1}\boldsymbol{\mu}_j,$$

where we denote by $\mathrm{diag}(\boldsymbol{L})$ the diagonal matrix with entries L_1, L_2 and L_3.

Output: approximate Fourier space parts of the forces $\boldsymbol{F}_\approx^{\mathrm{3d,F}}(j) \approx \boldsymbol{F}^{\mathrm{3d,F}}(j)$, $j = 1, \ldots, N$. $\square$

3 Periodic boundary conditions in two of three dimensions

We consider systems that are periodic only in the first two dimensions, i.e., we set $\mathcal{S} := \mathbb{Z}^2 \times \{0\}$ and define the energy

$$U^{\mathrm{2d}} := U_{\mathbb{Z}^2 \times \{0\}}$$

via (1.1). By applying the splitting (1.7) we end up as in the 3d-periodic case with the decomposition

$$U^{\mathrm{2d}} = U^{\mathrm{2d,short}} + U^{\mathrm{2d,long}} + U^{\mathrm{self}}$$

$$=: U_{\mathbb{Z}^2 \times \{0\}}^{\mathrm{short}} + U_{\mathbb{Z}^2 \times \{0\}}^{\mathrm{long}} + U^{\mathrm{self}}$$

via (1.8), (1.10) and (1.11), respectively.

The Fourier space representation of the long range part has already been derived in [16]. It is easy to see that the same Fourier space representation is obtained by replacing the charges q_j in the Ewald formula for Coulomb interactions by the operators $\boldsymbol{\mu}_j \cdot \nabla_{\boldsymbol{x}_j}$, see also [16]. By doing this we can formally write the Fourier space part of the energy as

$$U^{2\mathrm{d,long}} = U^{2\mathrm{d,F}} = \frac{1}{2L_1 L_2} \sum_{\boldsymbol{k} \in \mathbb{Z}^2} \sum_{i,j=1}^{N} (\boldsymbol{\mu}_i \cdot \nabla_{\boldsymbol{x}_i})(\boldsymbol{\mu}_j \cdot \nabla_{\boldsymbol{x}_j}) \Theta^{2\mathrm{d}}(\|\boldsymbol{k}\|, x_{ij,3}) \mathrm{e}^{2\pi \mathrm{i}(\boldsymbol{k} \oslash \tilde{\boldsymbol{L}}) \cdot \tilde{\boldsymbol{x}}_{ij}}, \quad (3.1)$$

where we use the notation

$$\boldsymbol{x}_j = (x_{j,1}, x_{j,2}, x_{j,3}) =: (\tilde{\boldsymbol{x}}_j, x_{j,3}), \quad \tilde{\boldsymbol{L}} := (L_1, L_2),$$

with $\tilde{\boldsymbol{x}}_j \in [-L_1/2, L_1/2] \times [-L_2/2, L_2/2]$ and the function $\Theta^{2\mathrm{d}}$ is defined via

$$\Theta^{2\mathrm{d}}(k, r) := \begin{cases} \dfrac{1}{2k} \left[\mathrm{e}^{2\pi k r} \mathrm{erfc}\left(\dfrac{\pi k}{\alpha} + \alpha r \right) + \mathrm{e}^{-2\pi k r} \mathrm{erfc}\left(\dfrac{\pi k}{\alpha} - \alpha r \right) \right] & : k \neq 0, \\ \dfrac{-2\sqrt{\pi}}{\alpha} \left(\mathrm{e}^{-\alpha^2 r^2} + \sqrt{\pi} \alpha r \, \mathrm{erf}(\alpha r) \right) & : k = 0. \end{cases} \quad (3.2)$$

Remark 3.1. In the 3d-periodic case the $\boldsymbol{k} = \boldsymbol{0}$ contribution as given in (2.3) has a very special form and thus we have to write the long range part of the energy as

$$U^{3\mathrm{d,long}} = U^{3\mathrm{d,F}} + U^{3\mathrm{d,0}},$$

i.e., we separate the $\boldsymbol{k} = \boldsymbol{0}$ term.

Also in the 2d-periodic case the $\boldsymbol{k} = \boldsymbol{0}$ contribution takes a slightly different form than in the case $\boldsymbol{k} \neq \boldsymbol{0}$. But by defining $\Theta^{2\mathrm{d}}$ as in (3.2) we are able to express the long range part as a single sum in Fourier space, see (3.1). In order to ensure consistency with the 3d-periodic case we introduce the double designation

$$U^{2\mathrm{d,long}} = U^{2\mathrm{d,F}},$$

see equation (3.1). $\qquad\square$

It is easy to show that we have $\Theta^{2\mathrm{d}}(k, r) = o(k^{-2}\mathrm{e}^{-k^2})$ as $k \to \infty$, see [25, Lemma 4.2], i.e., the infinite sum in (3.1) converges rapidly. Thus, we are able to replace the infinite sum over $\boldsymbol{k} \in \mathbb{Z}^2$ by a finite sum over $\boldsymbol{k} \in \mathcal{I}_{(M_1, M_2)}$, where we choose $M_1, M_2 \in 2\mathbb{N}$ large enough.

We follow the approach presented in [25, 26] and approximate the functions $\Theta^{2\mathrm{d}}(\|\boldsymbol{k}\|, \cdot)$ for all $\boldsymbol{k} \in \mathcal{I}_{(M_1, M_2)}$ by trigonometric polynomials. In the following we describe two different approaches to compute such a Fourier space approximation, namely the regularization approach, see [25, Section 4.2.1] for more details, as well as the periodization technique, which we already introduced in [26, Section 4]. After replacing the functions by their Fourier space approximations we apply the operators $\boldsymbol{\mu}_j \cdot \nabla_{\boldsymbol{x}_j}$, i.e., we follow a Fourier space differentiation approach at this point.

Regularization

Assuming that $x_{j,3} \in [-L_3/2, L_3/2]$ we obtain $x_{ij,3} \in [-L_3, L_3]$. Now, we proceed as follows.

i) We choose an interval length h, which fulfills $h > 2L_3$.

ii) For each $k = \|\boldsymbol{k}\|$, $\boldsymbol{k} \in \mathcal{I}_{(M_1, M_2)}$, we construct a polynomial $P(k, \cdot)$, which lives on the interval $[L_3, h - L_3]$ and interpolates the derivatives

$$\frac{\partial^n}{\partial r^n} \Theta^{2\mathrm{d}}(k, r)$$

at the end points $r = \pm L_3$ of the interval up to a certain order $p \in \mathbb{N}$, i.e., we construct $P(k, \cdot)$ such that

$$\frac{\partial^n}{\partial r^n} P(k, L_3) = \frac{\partial^n}{\partial r^n} \Theta^{2\mathrm{d}}(k, L_3) \quad \text{and} \quad \frac{\partial^n}{\partial r^n} P(k, h - L_3) = \frac{\partial^n}{\partial r^n} \Theta^{2\mathrm{d}}(k, -L_3)$$

for all $n = 0, \ldots, p$. The computation of the polynomial $P(k, \cdot)$ is possible via the two-point Taylor interpolation approach, see [1] or [13], for instance.

Then we define the regularized function $R(k, \cdot) \in C^p[-h/2, h/2]$ by

$$R(k, r) := \begin{cases} \Theta^{2\mathrm{d}}(k, r) & : |r| \leq L_3, \\ P(k, |r|) & : |r| > L_3. \end{cases}$$
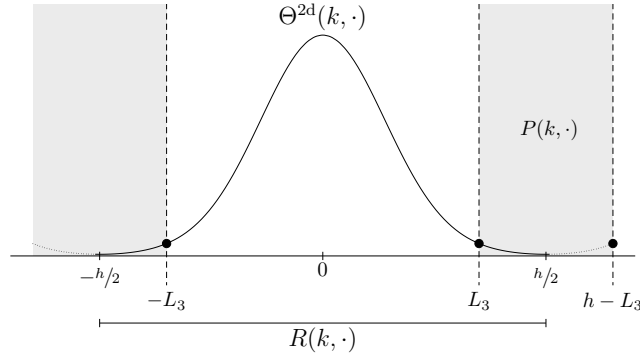
For a graphical illustration see Figure 3.1.

Figure 3.1: Example for a regularization $R(k, \cdot)$ for $k > 0$.

iii) The regularized functions $R(k, \cdot)$ are smooth on $[-h/2, h/2]$ and can thus be approximated by trigonometric polynomials

$$R(k, r) \approx \sum_{\ell \in \mathcal{I}_{M_3}} \hat{b}_{k, \ell} \mathrm{e}^{2\pi \mathrm{i} \ell r / h},$$

where we choose $M_3 \in 2\mathbb{N}$ large enough. The Fourier coefficients $\hat{b}_{k, \ell}$ are obtained by applying the FFT after sampling the function $R(k, \cdot)$ on an equispaced grid, i.e., we set

$$\hat{b}_{k, \ell} := \frac{1}{|\mathcal{I}_{M_3}|} \sum_{j \in \mathcal{I}_{M_3}} R(k, \tfrac{jh}{M_3}) \mathrm{e}^{-2\pi \mathrm{i} j \ell / M_3}, \quad \ell \in \mathcal{I}_{M_3}.$$

Since the function $R(k, \cdot)$ coincides with $\Theta^{2\mathrm{d}}(k, \cdot)$ on the interval $[-L_3, L_3]$ we have

$$\Theta^{2\mathrm{d}}(\|\boldsymbol{k}\|, x_{ij,3}) \approx \sum_{\ell \in \mathcal{I}_{M_3}} \hat{b}_{\|\boldsymbol{k}\|, \ell} \mathrm{e}^{2\pi \mathrm{i} \ell x_{ij,3} / h}. \tag{3.3}$$

Periodization

The Fourier transform of $\Theta^{2d}(k, r)$ with respect to r exists and is known in an analytically closed form for all $k > 0$. We obtain

$$\hat{\Theta}^{2d}(k, \xi) := \int_{-\infty}^{\infty} \Theta^{2d}(k, r)\mathrm{e}^{-2\pi \mathrm{i}r\xi}\mathrm{d}\xi = \frac{\mathrm{e}^{-\pi^2(k^2+\xi^2)/\alpha^2}}{\pi(k^2 + \xi^2)}, \tag{3.4}$$

which we easily compute by making use of the identity, cf. [25, Appendix A],

$$\Theta^{2d}(k, r) = 2\sqrt{\pi} \int_0^{\alpha} \frac{1}{z^2}\mathrm{e}^{-\pi^2 k^2/z^2 - r^2 z^2}\mathrm{d}z.$$

The function $\Theta^{2d}(0, \cdot)$ is non decreasing and thus the Fourier transform does not exist. In other words, at least in the case $k = 0$ we need to apply the regularization approach as described above. For $k \neq 0$ we can use the analytical Fourier transform as given in (3.4) as follows.

If $k > 0$ is large enough we expect that we only make a negligible error when approximating the function $\Theta^{2d}(k, \cdot)$ by its h-periodic version, i.e., we have

$$\Theta^{2d}(k, r) \approx \sum_{n\in\mathbb{Z}} \Theta^{2d}(k, r + hn) \tag{3.5}$$

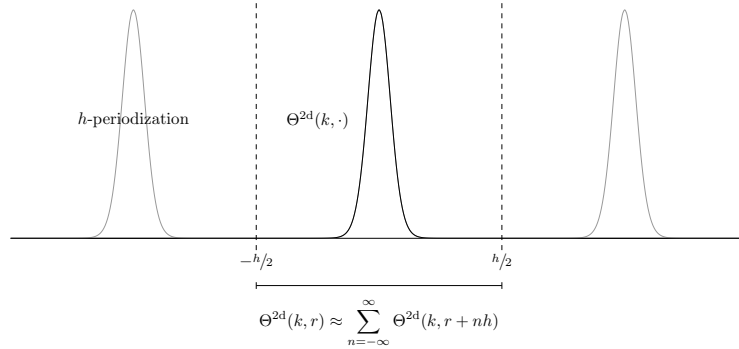for all $r \in [-L_3, L_3] \subset [-h/2, h/2]$, see Figure 3.2.

Figure 3.2: Approximation of $\Theta^{2d}(k, \cdot)$, $k > 0$, by its h-periodization.

Via the Poisson summation formula and truncation in Fourier space, which is possible since the Fourier transform (3.4) tends to zero exponentially fast in ξ, we obtain

$$\Theta^{2d}(k, r) \approx \sum_{n\in\mathbb{Z}} \Theta^{2d}(k, r + hn) = \frac{1}{h}\sum_{\ell\in\mathbb{Z}} \hat{\Theta}^{2d}(k, \ell/h)\mathrm{e}^{2\pi\mathrm{i}\ell r/h} \approx \frac{1}{h}\sum_{\ell\in\mathcal{I}_{M_3}} \hat{\Theta}^{2d}(k, \ell/h)\mathrm{e}^{2\pi\mathrm{i}\ell r/h},$$

i.e., we simply set $\hat{b}_{k,\ell} := \frac{1}{h}\hat{\Theta}^{2d}(k, \ell/h)$ and end up with an approximation of the form (3.3).

Note that this approach is equivalent to truncating the integral

$$\Theta^{2d}(k, r) = \int_{\mathbb{R}} \hat{\Theta}^{2d}(k, \xi)\mathrm{e}^{2\pi\mathrm{i}r\xi}\mathrm{d}\xi$$

and approximating the remaining finite integral via the trapezoidal quadrature rule, which is the basic idea of the 2d-periodic fast and spectrally accurate Ewald summation [22] for Coulomb interactions.

3.1 Computation of the electrostatic fields and torques

In a precomputation step we compute the coefficients $\hat{b}_{\|\boldsymbol{k}\|,\ell}$ such that we have for each $\boldsymbol{k} \in \mathcal{I}_{(M_1,M_2)}$ an approximation of the form (3.3). Thereby, we use the same cutoff M_3 as well as the same period h for all $\boldsymbol{k}$. The approximations are obtained by

i) regularizing the function in the case $\|\boldsymbol{k}\| = 0$ or $\|\boldsymbol{k}\| \neq 0$ small,

ii) periodizing the function if $\|\boldsymbol{k}\| \neq 0$ is large enough,

as described above.

Note that this precomputation step only depends on the box length L_3 in the nonperiodic dimension and not on the positions $\boldsymbol{x}_j$ of the dipoles themselves. This means that the precomputations have to be done only once if the particles do not leave the box with respect to the nonperiodic coordinate during a simulation. If at least one particle leaves the box, the precomputations have to be done again. Thus, the value for L_3 should always be chosen somewhat larger than actually necessary.

Remark 3.2. The combination of the above described regularization and periodization approaches serves several advantages.

On the one hand, the regularization approach does not require a localization or rather decrease of the kernel function $\Theta^{2\mathrm{d}}(k,\cdot)$. This is especially crucial in the case $k = 0$. Additionally, for $k \neq 0$ we are able to embed $\Theta^{2\mathrm{d}}(k,\cdot)$ into a periodic function whose period h is not too large compared to the double box length $2L_3$. Especially for small values of k we would have to choose a very large period h in order to approximate the function by its periodization (3.5), which would also lead to a larger number M_3 of required approximating terms. On the other hand, the amount of precomputations is larger for the regularization technique, since for each k we have to compute the interpolating polynomial $P(k,\cdot)$ and compute the coefficients $\hat{b}_{k,\ell}$ by using the FFT, for which the regularized kernel $R(k,\cdot)$ has to be sampled on an equispaced grid.

Less precomputations are required for the periodization approach since the corresponding Fourier coefficients are known analytically, but the function has to be sufficiently small outside the interval $[-^h/_2, ^h/_2]$. Furthermore, the approximating function is in $C^\infty(\mathbb{R})$ and not only smooth of order $p \in \mathbb{N}$ as it is the case for the regularized kernels $R(k,\cdot)$.

Combining the two approaches serves a compromise between the required amount of precomputations and the needed number of grid points M_3 in the nonperiodic dimension. The same is possible in the 1d-periodic setting, see Section 4.

Note that the mixed periodic case, using these two approximation techniques in the precomputation step, has already been implemented for Coulomb interactions, cf. [25] and [26]. The software is publicly available as a part of the ScaFaCoS library [2]. For numerical results see [25, Section 4.3] for the 2d-periodic case and [25, Section 5.3] for the 1d-periodic case. $\square$

Having the approximations (3.3) for all vectors $\boldsymbol{k} \in \mathcal{I}_{(M_1,M_2)}$, the electrostatic fields can be approximated analogously to the 3d-periodic case.

From the Ewald formulas for the energy $U^{2\mathrm{d}}$, which we describe at the very beginning of Section 3, we easily obtain the Ewald formulas for the fields $\boldsymbol{E}^{2\mathrm{d}}(j)$ via (1.5). The splitting of the electrostatic fields reads as

$$\boldsymbol{E}^{2\mathrm{d}}(j) = \boldsymbol{E}^{2\mathrm{d,short}}(j) + \boldsymbol{E}^{2\mathrm{d,F}}(j) + \boldsymbol{E}^{\mathrm{self}}(j),$$

where the short range parts $\boldsymbol{E}^{2\text{d,short}}(j) := \boldsymbol{E}^{\text{short}}_{\mathbb{Z}^2 \times \{0\}}(j)$ are defined via (2.4) and the self interaction term $\boldsymbol{E}^{\text{self}}(j)$ is given by (2.8). Using an appropriate far field cutoff $(M_1, M_2) \in 2\mathbb{N}^2$ and the approximations (3.3) we obtain for the Fourier space parts

$$
\begin{aligned}
\boldsymbol{E}^{2\text{d,F}}(j) &\approx -\frac{\nabla_{\boldsymbol{x}_j}}{L_1 L_2} \sum_{\boldsymbol{k} \in \mathcal{I}_{(M_1, M_2)}} \sum_{i=1}^{N} (\boldsymbol{\mu}_i \cdot \nabla_{\boldsymbol{x}_i}) \Theta^{2\text{d}}(\|\boldsymbol{k}\|, x_{ij,3}) \mathrm{e}^{2\pi\mathrm{i}(\boldsymbol{k} \oslash \tilde{\boldsymbol{L}}) \cdot \tilde{\boldsymbol{x}}_{ij}} \\
&\approx -\frac{\nabla_{\boldsymbol{x}_j}}{L_1 L_2} \sum_{(\boldsymbol{k},\ell) \in \mathcal{I}_{\boldsymbol{M}}} \hat{b}_{\|\boldsymbol{k}\|,\ell} \left(\sum_{i=1}^{N} (\boldsymbol{\mu}_i \cdot \nabla_{\boldsymbol{x}_i}) \mathrm{e}^{2\pi\mathrm{i}\begin{pmatrix}\boldsymbol{k} \oslash \tilde{\boldsymbol{L}} \\ \ell/h\end{pmatrix} \cdot \boldsymbol{x}_i} \right) \mathrm{e}^{-2\pi\mathrm{i}\begin{pmatrix}\boldsymbol{k} \oslash \tilde{\boldsymbol{L}} \\ \ell/h\end{pmatrix} \cdot \boldsymbol{x}_j} \\
&= -\frac{4\pi^2}{L_1 L_2} \sum_{(\boldsymbol{k},\ell) \in \mathcal{I}_{\boldsymbol{M}}} \hat{b}_{\|\boldsymbol{k}\|,\ell} \begin{pmatrix}\boldsymbol{k} \oslash \tilde{\boldsymbol{L}} \\ \ell/h\end{pmatrix} \left[\begin{pmatrix}\boldsymbol{k} \oslash \tilde{\boldsymbol{L}} \\ \ell/h\end{pmatrix} \cdot \boldsymbol{S}(\boldsymbol{k},\ell) \right] \mathrm{e}^{-2\pi\mathrm{i}\begin{pmatrix}\boldsymbol{k} \oslash \tilde{\boldsymbol{L}} \\ \ell/h\end{pmatrix} \cdot \boldsymbol{x}_j},
\end{aligned}
\tag{3.6}
$$

where we set $\boldsymbol{M} := (M_1, M_2, M_3) \in 2\mathbb{N}^3$ and

$$
\boldsymbol{S}(\boldsymbol{k}, \ell) := \sum_{i=1}^{N} \boldsymbol{\mu}_i \mathrm{e}^{2\pi\mathrm{i}\begin{pmatrix}\boldsymbol{k} \oslash \tilde{\boldsymbol{L}} \\ \ell/h\end{pmatrix} \cdot \boldsymbol{x}_i}.
$$

The efficient approximation of the Fourier space parts $\boldsymbol{E}^{2\text{d,F}}(j) \approx \boldsymbol{E}^{2\text{d,F}}_{\approx}(j)$ can be done as in the 3d-periodic case via Algorithm (2.1) (i$\boldsymbol{k}$-differentiation) or via Algorithm (2.2) (analytic differentiation), where we formally replace

$$
\frac{1}{V} \hat{\psi}(\boldsymbol{k}), \boldsymbol{k} \in \mathcal{I}_{\boldsymbol{M}}, \quad \text{by} \quad \frac{\pi}{L_1 L_2} \hat{b}_{\|\boldsymbol{k}\|,\ell}, (\boldsymbol{k}, \ell) \in \mathcal{I}_{\boldsymbol{M}}
\tag{3.7}
$$

and

$$
\boldsymbol{k} \oslash \boldsymbol{L} \in \mathbb{R}^3 \quad \text{by} \quad \begin{pmatrix}\boldsymbol{k} \oslash \tilde{\boldsymbol{L}} \\ \ell/h\end{pmatrix} \in \mathbb{R}^3.
\tag{3.8}
$$

As already mentioned in Section 2, the short range parts can be approximated by $\boldsymbol{E}^{2\text{d,short}}_{\approx}(j)$ via a direct evaluation. Finally, we obtain the approximations of the single fields by

$$
\boldsymbol{E}^{2\text{d}}_{\approx}(j) := \boldsymbol{E}^{2\text{d,short}}_{\approx}(j) + \boldsymbol{E}^{2\text{d,F}}_{\approx}(j) + \boldsymbol{E}^{\text{self}}(j).
$$

Based on the computed approximations of the fields $\boldsymbol{E}^{2\text{d}}_{\approx}(j)$ the torques are simply obtained by (1.3), i.e., we set

$$
\boldsymbol{\tau}^{2\text{d}}(j) \approx \boldsymbol{\tau}^{2\text{d}}_{\approx}(j) := \boldsymbol{\mu}_j \times \boldsymbol{E}^{2\text{d}}_{\approx}(j).
$$

An approximation of the energy $U^{2\text{d}}$ is obtained via

$$
U^{2\text{d}}_{\approx} := -\frac{1}{2} \sum_{j=1}^{N} \boldsymbol{\mu}_j \cdot \boldsymbol{E}^{2\text{d}}_{\approx}(j),
$$

following the identity (1.5).

3.2 Computation of the forces

The Ewald formulas for the forces $\boldsymbol{F}^{2\mathrm{d}}(j)$ are obtained via (1.6), i.e.,

$$\boldsymbol{F}^{2\mathrm{d}}(j) = \nabla_{\boldsymbol{x}_j}\left[\boldsymbol{\mu}_j \cdot \boldsymbol{E}^{2\mathrm{d}}(j)\right] = \boldsymbol{F}^{2\mathrm{d,short}}(j) + \boldsymbol{F}^{2\mathrm{d,F}}(j),$$

where the short range parts $\boldsymbol{F}^{2\mathrm{d,short}}(j) := \boldsymbol{F}^{\mathrm{short}}_{\mathbb{Z}^2\times\{0\}}(j)$ are defined via (2.10) and can be computed directly.

For the Fourier space parts we obtain from (3.6)

$$\boldsymbol{F}^{2\mathrm{d,F}} \approx -\frac{\nabla_{\boldsymbol{x}_j}(\boldsymbol{\mu}_j \cdot \nabla_{\boldsymbol{x}_j})}{L_1 L_2} \sum_{\boldsymbol{k}\in\mathcal{I}_{(M_1,M_2)}} \sum_{i=1}^{N}(\boldsymbol{\mu}_i \cdot \nabla_{\boldsymbol{x}_i})\Theta^{2\mathrm{d}}(\|\boldsymbol{k}\|, x_{ij,3})\mathrm{e}^{2\pi\mathrm{i}(\boldsymbol{k}\oslash\boldsymbol{L})\cdot\tilde{\boldsymbol{x}}_{ij}}$$

$$\approx -\frac{\nabla_{\boldsymbol{x}_j}(\boldsymbol{\mu}_j \cdot \nabla_{\boldsymbol{x}_j})}{L_1 L_2} \sum_{(\boldsymbol{k},\ell)\in\mathcal{I}_M} \hat{b}_{\|\boldsymbol{k}\|,\ell}\left(\sum_{i=1}^{N}(\boldsymbol{\mu}_i \cdot \nabla_{\boldsymbol{x}_i})\mathrm{e}^{2\pi\mathrm{i}\binom{\boldsymbol{k}\oslash\tilde{\boldsymbol{L}}}{\ell/h}\cdot\boldsymbol{x}_i}\right)\mathrm{e}^{-2\pi\mathrm{i}\binom{\boldsymbol{k}\oslash\tilde{\boldsymbol{L}}}{\ell/h}\cdot\boldsymbol{x}_j}$$

$$= \frac{8\pi^3\mathrm{i}}{L_1 L_2} \sum_{(\boldsymbol{k},\ell)\in\mathcal{I}_M} \hat{b}_{\|\boldsymbol{k}\|,\ell}\left[\boldsymbol{\mu}_j \cdot \binom{\boldsymbol{k}\oslash\tilde{\boldsymbol{L}}}{\ell/h}\right]\left[\binom{\boldsymbol{k}\oslash\tilde{\boldsymbol{L}}}{\ell/h} \cdot \boldsymbol{S}(\boldsymbol{k},\ell)\right]\binom{\boldsymbol{k}\oslash\tilde{\boldsymbol{L}}}{\ell/h}\mathrm{e}^{-2\pi\mathrm{i}\binom{\boldsymbol{k}\oslash\tilde{\boldsymbol{L}}}{\ell/h}\cdot\boldsymbol{x}_j}$$

$$= \frac{8\pi^3\mathrm{i}}{L_1 L_2} \sum_{(\boldsymbol{k},\ell)\in\mathcal{I}_M} \hat{b}_{\|\boldsymbol{k}\|,\ell}\binom{\boldsymbol{k}\oslash\tilde{\boldsymbol{L}}}{\ell/h}\binom{\boldsymbol{k}\oslash\tilde{\boldsymbol{L}}}{\ell/h}^{\top}\left[\binom{\boldsymbol{k}\oslash\tilde{\boldsymbol{L}}}{\ell/h} \cdot \boldsymbol{S}(\boldsymbol{k},\ell)\right]\boldsymbol{\mu}_j\mathrm{e}^{-2\pi\mathrm{i}\binom{\boldsymbol{k}\oslash\tilde{\boldsymbol{L}}}{\ell/h}\cdot\boldsymbol{x}_j}.$$

The efficient computation of the Fourier space parts $\boldsymbol{F}^{2\mathrm{d,F}}(j)$ can be done analogously to the 3d-periodic case via Algorithm (2.3) (i$\boldsymbol{k}$-differentiation) or via Algorithm (2.4) (analytic differentiation), where we make the replacements (3.7) and (3.8).

4 Periodic boundary conditions in one of three dimensions

We consider systems that are periodic only in the first dimension, i.e., we set $\mathcal{S} := \mathbb{Z}\times\{0\}^2$ and define the energy

$$U^{1\mathrm{d}} := U_{\mathbb{Z}\times\{0\}^2}.$$

As in the 2d-periodic case the energy can be written as

$$U^{1\mathrm{d}} = U^{1\mathrm{d,short}} + U^{1\mathrm{d,long}} + U^{\mathrm{self}}$$

$$=: U^{\mathrm{short}}_{\mathbb{Z}\times\{0\}^2} + U^{\mathrm{long}}_{\mathbb{Z}\times\{0\}^2} + U^{\mathrm{self}}$$

via (1.8), (1.10) and (1.11), respectively.

The Fourier space representation of the long range part has already been derived in [29]. It is easy to see that the same Fourier space representation is obtained by replacing the charges q_j in the Ewald formula for Coulomb interactions by the operators $\boldsymbol{\mu}_j \cdot \nabla_{\boldsymbol{x}_j}$, see also [29]. By doing this we can formally write the Fourier space part of the energy as

$$U^{1\mathrm{d,long}} = U^{1\mathrm{d,F}} = \frac{1}{2L_1} \sum_{k\in\mathbb{Z}} \sum_{i,j=1}^{N}(\boldsymbol{\mu}_i \cdot \nabla_{\boldsymbol{x}_i})(\boldsymbol{\mu}_j \cdot \nabla_{\boldsymbol{x}_j})\Theta^{1\mathrm{d}}(k, x_{ij,3})\mathrm{e}^{2\pi\mathrm{i}(k/L_1)\cdot x_{ij,1}}, \qquad (4.1)$$

where we use the notation

$$\boldsymbol{x}_j = (x_{j,1}, x_{j,2}, x_{j,3}) =: (x_{j,1}, \tilde{\boldsymbol{x}}_j),$$

and the function $\Theta^{1\mathrm{d}}$ is defined via

$$\Theta^{1\mathrm{d}}(k, r) := \begin{cases} K_0\left(\frac{\pi^2 k^2}{\alpha^2}, \alpha^2 r^2\right) & : k \neq 0, \\ -\gamma - \Gamma(0, \alpha^2 r^2) - \ln(\alpha^2 r^2) & : k = 0. \end{cases}$$

Thereby, γ is the Euler-Mascheroni constant,

$$K_s(x, y) := \int_1^\infty t^{-s-1} \mathrm{e}^{-xt - y/t} \mathrm{d}t$$

is the incomplete modified Bessel function of the second kind, see [17] for more information, and

$$\Gamma(s, x) := \int_x^\infty t^{s-1} \mathrm{e}^{-t} \mathrm{d}t$$

is the upper incomplete Gamma function, which can also be expressed in terms of the well known exponential integral function in the case $s = 0$.

It is easy to show that $\Theta^{1\mathrm{d}}(k, r) = o(k^{-2} \mathrm{e}^{-k^2})$ as $k \to \infty$, see [25, Lemma 5.2], i.e., the infinite sum in (4.1) converges rapidly. Thus, we can simply replace the infinite sum over $k \in \mathbb{Z}$ by a finite sum over $k \in \mathcal{I}_{M_1}$, where we choose $M_1 \in 2\mathbb{N}$ large enough.

Again, we follow the approach presented in [25, 26] and approximate the functions $\Theta^{1\mathrm{d}}(k, \cdot)$ for all $k \in \mathcal{I}_{M_1}$ by trigonometric polynomials, where we apply the operators $\boldsymbol{\mu}_j \cdot \nabla_{\boldsymbol{x}_j}$ after replacing the functions by their precomputed Fourier space approximations.

Regularization

The regularization has to be done somewhat different to the 2d-periodic case since we now have to deal with bivariate functions.

Assuming that $\tilde{\boldsymbol{x}}_j \in [-L_2/2, L_2/2] \times [-L_3/2, L_3/2]$ we have $\|\tilde{\boldsymbol{x}}_{ij}\| \leq \sqrt{L_2^2 + L_3^2}$ and we can proceed as follows.

i) We choose an interval length $h > 2\sqrt{L_2^2 + L_3^2}$.

ii) For each $k \in \mathcal{I}_{M_1}$ we construct a polynomial $P(k, \cdot)$, which lives on the interval $[\sqrt{L_2^2 + L_3^2}, h/2]$ and interpolates the derivatives of $\Theta^{1\mathrm{d}}(k, r)$ with respect to r at $r = \sqrt{L_2^2 + L_3^2}$ and has vanishing derivatives at $r = h/2$ up to a certain degree $p \in \mathbb{N}$, i.e., we construct $P(k, \cdot)$ such that

$$\frac{\partial^n}{\partial r^n} P(k, \sqrt{L_2^2 + L_3^2}) = \frac{\partial^n}{\partial r^n} \Theta^{1\mathrm{d}}(k, \sqrt{L_2^2 + L_3^2})$$

for all $n = 0, \ldots, p$ and

$$\frac{\partial^n}{\partial r^n} P(k, h/2) = 0$$

for all $n = 1, \ldots, p$. The computation of the polynomial $P(k, \cdot)$ is possible via a modified two-point Taylor interpolation approach, which we describe in [25, Appendix C]. Then

we define the regularized function $R(k, \cdot) \in C^p[-h/2, h/2]^2$ for $\boldsymbol{y} \in [-h/2, h/2]^2$ by

$$R(k, \boldsymbol{y}) := \begin{cases} \Theta^{1\mathrm{d}}(k, \|\boldsymbol{y}\|) & : \|\boldsymbol{y}\| \le \sqrt{L_2^2 + L_3^2}, \\ P(k, \|\boldsymbol{y}\|) & : \sqrt{L_2^2 + L_3^2} < \|\boldsymbol{y}\| \le h/2, \\ P(k, h/2) & : \|\boldsymbol{y}\| > h/2. \end{cases}$$
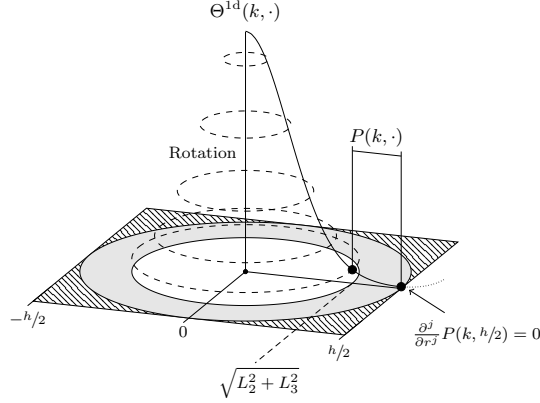
For a graphical illustration see Figure 4.1.

Figure 4.1: Example for regularizing $\Theta^{1\mathrm{d}}(k, \cdot)$ for $k > 0$.

iii) The regularized functions $R(k, \cdot)$ are smooth on $[-h/2, h/2]^2$ and can thus be approximated by bivariate trigonometric polynomials

$$R(k, \boldsymbol{y}) \approx \sum_{\boldsymbol{\ell} \in \mathcal{I}_{\tilde{\boldsymbol{M}}}} \hat{b}_{|k|, \boldsymbol{\ell}} \mathrm{e}^{2\pi\mathrm{i}(\boldsymbol{\ell}/h) \cdot \boldsymbol{y}},$$

where we choose $\tilde{\boldsymbol{M}} \in 2\mathbb{N}^2$ large enough. The Fourier coefficients are obtained by applying the FFT after sampling the function $R(k, \cdot)$ on a two-dimensional equispaced grid, i.e., we set

$$\hat{b}_{k, \boldsymbol{\ell}} := \frac{1}{|\mathcal{I}_{\tilde{\boldsymbol{M}}}|} \sum_{\boldsymbol{j} \in \mathcal{I}_{\tilde{\boldsymbol{M}}}} R(k, (\boldsymbol{j} \oslash \tilde{\boldsymbol{M}})h) \mathrm{e}^{-2\pi\mathrm{i}(\boldsymbol{j} \oslash \tilde{\boldsymbol{M}}) \cdot \boldsymbol{\ell}}, \quad \boldsymbol{\ell} \in \mathcal{I}_{\tilde{\boldsymbol{M}}}.$$

Since $R(k, \boldsymbol{y}) = \Theta^{1\mathrm{d}}(k, \|\boldsymbol{y}\|)$ for all $\boldsymbol{y} \in \mathbb{R}^2 : \|\boldsymbol{y}\| \le \sqrt{L_2^2 + L_3^2}$ we have

$$\Theta^{1\mathrm{d}}(k, \|\tilde{\boldsymbol{x}}_{ij}\|) \approx \sum_{\boldsymbol{\ell} \in \mathcal{I}_{\tilde{\boldsymbol{M}}}} \hat{b}_{|k|, \boldsymbol{\ell}} \mathrm{e}^{2\pi\mathrm{i}(\boldsymbol{\ell}/h) \cdot \tilde{\boldsymbol{x}}_{ij}}. \tag{4.2}$$

Note that the evaluation of the incomplete modified Bessel function K_0 and their derivatives raises several numerical difficulties. The method presented in [31] is one of very few publicly available algorithms for the evaluation of the incomplete modified Bessel function. In the P^{2}NFFT method for 1d-periodic boundary conditions we use this iterative algorithm with some modifications in order to overcome numerical instabilities in certain cases, see [25, Section 5.2.2].

Periodization

The Fourier transform of the radial function $\Theta^{1\mathrm{d}}(k, \|\boldsymbol{y}\|)$ with respect to $\boldsymbol{y} \in \mathbb{R}^2$ exists and is known in an analytically closed form for all $k > 0$. We obtain

$$\int_{\mathbb{R}^2} \Theta^{1\mathrm{d}}(k, \|\boldsymbol{y}\|)\mathrm{e}^{-2\pi\mathrm{i}\boldsymbol{y}\cdot\boldsymbol{\xi}}\mathrm{d}\boldsymbol{y} = \frac{\mathrm{e}^{-\pi^2(k^2+\|\boldsymbol{\xi}\|^2)/\alpha^2}}{\pi(k^2+\|\boldsymbol{\xi}\|^2)} =: \hat{\Theta}^{1\mathrm{d}}(k, \xi),$$

where we set $\xi := \|\boldsymbol{\xi}\|$. As in the 2d-periodic case, the function $\Theta^{1\mathrm{d}}(0, \cdot)$ is non decreasing, i.e., the Fourier transform does not exist and we have to follow the regularization approach.

If $k > 0$ is large enough we expect that the function $\Theta^{1\mathrm{d}}(k, \cdot)$ is well approximated by its bivariate h-periodization, i.e., we have

$$\Theta^{1\mathrm{d}}(k, \|\boldsymbol{y}\|) \approx \sum_{\boldsymbol{n}\in\mathbb{Z}^2} \Theta^{1\mathrm{d}}(k, \|\boldsymbol{y} + h\boldsymbol{n}\|),$$

for all $\{\boldsymbol{y} \in \mathbb{R}^2 : \|\boldsymbol{y}\| \leq \sqrt{L_2^2 + L_3^2}\} \subset [-h/2, h/2]^2$.

Via the Poisson summation formula we obtain

$$\Theta^{1\mathrm{d}}(k, \|\boldsymbol{y}\|) \approx \sum_{\boldsymbol{n}\in\mathbb{Z}^2} \Theta^{1\mathrm{d}}(k, \|\boldsymbol{y} + h\boldsymbol{n}\|) = \frac{1}{h^2} \sum_{\boldsymbol{\ell}\in\mathbb{Z}^2} \hat{\Theta}^{1\mathrm{d}}(k, h^{-1}\|\boldsymbol{\ell}\|)\mathrm{e}^{2\pi\mathrm{i}(\boldsymbol{\ell}/h)\cdot\boldsymbol{y}}$$

$$\approx \frac{1}{h^2} \sum_{\boldsymbol{\ell}\in\mathcal{I}_{\tilde{\boldsymbol{M}}}} \hat{\Theta}^{1\mathrm{d}}(k, h^{-1}\|\boldsymbol{\ell}\|)\mathrm{e}^{2\pi\mathrm{i}(\boldsymbol{\ell}/h)\cdot\boldsymbol{y}},$$

i.e., we end up with an approximation of the form (4.2).

4.1 Computation of the electrostatic fields and torques

In a precomputation step we compute the coefficients $\hat{b}_{|k|,\boldsymbol{\ell}}$ such that we have for each $k \in \mathcal{I}_{M_1}$ an approximation of the form (4.2). Thereby, we use the same cutoff $\tilde{\boldsymbol{M}}$ as well as the same period h for all k. The approximations are obtained by

i) regularizing the function in the case $k = 0$ or $|k| \neq 0$ small,

ii) periodizing the function if $|k| \neq 0$ is large enough,

as described above. Analogously to the 2d-periodic case, the described precomputation step only depends on the box lengths L_2, L_3 in the nonperiodic dimensions and not on the positions $\boldsymbol{x}_j$ of the dipoles. Thus, the precomputations have to be done only once if the particles do not leave the box with respect to the nonperiodic coordinates.

Having the approximations (4.2) for all $k \in \mathcal{I}_{M_1}$, the electrostatic fields can be approximated analogously to the 3d-periodic case.

From the Ewald formulas for the the energy $U^{1\mathrm{d}}$, which we describe at the very beginning of Section 4, the Ewald formulas for the fields $\boldsymbol{E}^{1\mathrm{d}}(j)$ are obtained easily via (1.5). The splitting of the electrostatic fields reads as

$$\boldsymbol{E}^{1\mathrm{d}}(j) = \boldsymbol{E}^{1\mathrm{d,short}}(j) + \boldsymbol{E}^{1\mathrm{d,F}}(j) + \boldsymbol{E}^{\mathrm{self}}(j),$$

where the short range parts $\boldsymbol{E}^{1\mathrm{d,short}}(j) := \boldsymbol{E}^{\mathrm{short}}_{\mathbb{Z}\times\{0\}^2}(j)$ are defined via (2.4) and the self interaction term $\boldsymbol{E}^{\mathrm{self}}(j)$ is given by (2.8).

Using an appropriate far field cutoff $M_1 \in 2\mathbb{N}$ and the approximations (4.2) we obtain for the Fourier space parts

$$\boldsymbol{E}^{\mathrm{1d,F}}(j) \approx -\frac{\nabla_{\boldsymbol{x}_j}}{L_1} \sum_{k \in \mathcal{I}_{M_1}} \sum_{i=1}^{N} (\boldsymbol{\mu}_i \cdot \nabla_{\boldsymbol{x}_i}) \Theta^{\mathrm{1d}}(|k\,\|\tilde{\boldsymbol{x}}_{ij}\||) \mathrm{e}^{2\pi\mathrm{i}(k/L_1)\boldsymbol{x}_{ij,1}}$$

$$\approx -\frac{\nabla_{\boldsymbol{x}_j}}{L_1} \sum_{(k,\boldsymbol{\ell}) \in \mathcal{I}_{\boldsymbol{M}}} \hat{b}_{|k|,\boldsymbol{\ell}} \left(\sum_{i=1}^{N} (\boldsymbol{\mu}_i \cdot \nabla_{\boldsymbol{x}_i}) \mathrm{e}^{2\pi\mathrm{i}\binom{k/L_1}{\boldsymbol{\ell}/h} \cdot \boldsymbol{x}_i} \right) \mathrm{e}^{-2\pi\mathrm{i}\binom{k/L_1}{\boldsymbol{\ell}/h} \cdot \boldsymbol{x}_j} \tag{4.3}$$

$$= -\frac{4\pi^2}{L_1} \sum_{(k,\boldsymbol{\ell}) \in \mathcal{I}_{\boldsymbol{M}}} \hat{b}_{|k|,\boldsymbol{\ell}} \binom{k/L_1}{\boldsymbol{\ell}/h} \left[\binom{k/L_1}{\boldsymbol{\ell}/h} \cdot \boldsymbol{S}(k,\boldsymbol{\ell}) \right] \mathrm{e}^{-2\pi\mathrm{i}\binom{k/L_1}{\boldsymbol{\ell}/h} \cdot \boldsymbol{x}_j},$$

where we set $\boldsymbol{M} := (M_1, \tilde{\boldsymbol{M}}) \in 2\mathbb{N}^3$ and

$$\boldsymbol{S}(k,\boldsymbol{\ell}) := \sum_{i=1}^{N} \boldsymbol{\mu}_i \mathrm{e}^{2\pi\mathrm{i}\binom{k/L_1}{\boldsymbol{\ell}/h} \cdot \boldsymbol{x}_i}.$$

The efficient computation of the Fourier space parts $\boldsymbol{E}^{\mathrm{1d,F}}(j)$ is done as in the 3d-periodic case via Algorithm (2.1) ($\mathrm{i}\boldsymbol{k}$-differentiation) or via Algorithm (2.2) (analytic differentiation), where we formally replace

$$\frac{1}{V}\hat{\psi}(\boldsymbol{k}), \boldsymbol{k} \in \mathcal{I}_{\boldsymbol{M}}, \quad \text{by} \quad \frac{\pi}{L_1}\hat{b}_{|k|,\boldsymbol{\ell}}, (k,\boldsymbol{\ell}) \in \mathcal{I}_{\boldsymbol{M}} \tag{4.4}$$

and

$$\boldsymbol{k} \oslash \boldsymbol{L} \in \mathbb{R}^3 \quad \text{by} \quad \binom{k/L_1}{\boldsymbol{\ell}/h} \in \mathbb{R}^3. \tag{4.5}$$

As described above, we can compute an approximation of the short range part $\boldsymbol{E}_{\approx}^{\mathrm{1d,short}}(j)$ by a direct summation. We denote the approximated fields by

$$\boldsymbol{E}_{\approx}^{\mathrm{1d}}(j) := \boldsymbol{E}_{\approx}^{\mathrm{1d,short}}(j) + \boldsymbol{E}_{\approx}^{\mathrm{1d,long}}(j) + \boldsymbol{E}^{\mathrm{self}}(j).$$

Based on the computed approximations of the fields $\boldsymbol{E}_{\approx}^{\mathrm{1d}}(j)$ the torques are simply obtained by (1.3), i.e., we approximate the torques by

$$\boldsymbol{\tau}^{\mathrm{1d}}(j) \approx \boldsymbol{\tau}_{\approx}^{\mathrm{1d}}(j) := \boldsymbol{\mu}_j \times \boldsymbol{E}_{\approx}^{\mathrm{1d}}(j).$$

An approximation of the energy U^{1d} is given by

$$U_{\approx}^{\mathrm{1d}} := -\frac{1}{2} \sum_{j=1}^{N} \boldsymbol{\mu}_j \cdot \boldsymbol{E}_{\approx}^{\mathrm{1d}}(j),$$

following the identity (1.5).

4.2 Computation of the forces

The Ewald formulas for the forces $\boldsymbol{F}^{1d}(j)$ are obtained by applying (1.6), i.e.,

$$\boldsymbol{F}^{1d}(j) = \nabla_{\boldsymbol{x}_j}\left[\boldsymbol{\mu}_j \cdot \boldsymbol{E}^{1d}(j)\right] = \boldsymbol{F}^{1d,\text{short}}(j) + \boldsymbol{F}^{1d,F}(j),$$

where the short range parts $\boldsymbol{F}^{1d,\text{short}}(j) := \boldsymbol{F}^{\text{short}}_{\mathbb{Z}\times\{0\}^2}(j)$ are defined via (2.10) and can be computed directly.

For the Fourier space parts we obtain from (4.3)

$$\boldsymbol{F}^{1d,F} \approx -\frac{\nabla_{\boldsymbol{x}_j}(\boldsymbol{\mu}_j \cdot \nabla_{\boldsymbol{x}_j})}{L_1}\sum_{k\in\mathcal{I}_{M_1}}\sum_{i=1}^{N}(\boldsymbol{\mu}_i \cdot \nabla_{\boldsymbol{x}_i})\Theta^{1d}(\|\boldsymbol{k}\|,\|\tilde{\boldsymbol{x}}_{ij}\|)\mathrm{e}^{2\pi\mathrm{i}(k/L_1)\cdot x_{ij,1}}$$

$$\approx -\frac{\nabla_{\boldsymbol{x}_j}(\boldsymbol{\mu}_j \cdot \nabla_{\boldsymbol{x}_j})}{L_1}\sum_{(k,\boldsymbol{\ell})\in\mathcal{I}_{\boldsymbol{M}}}\hat{b}_{|k|,\boldsymbol{\ell}}\left(\sum_{i=1}^{N}(\boldsymbol{\mu}_i \cdot \nabla_{\boldsymbol{x}_i})\mathrm{e}^{2\pi\mathrm{i}\begin{pmatrix}k/L_1\\\boldsymbol{\ell}/h\end{pmatrix}\cdot\boldsymbol{x}_i}\right)\mathrm{e}^{-2\pi\mathrm{i}\begin{pmatrix}k/L_1\\\boldsymbol{\ell}/h\end{pmatrix}\cdot\boldsymbol{x}_j}$$

$$= \frac{8\pi^3\mathrm{i}}{L_1}\sum_{(k,\boldsymbol{\ell})\in\mathcal{I}_{\boldsymbol{M}}}\hat{b}_{|k|,\boldsymbol{\ell}}\left[\boldsymbol{\mu}_j\cdot\begin{pmatrix}k/L_1\\\boldsymbol{\ell}/h\end{pmatrix}\right]\left[\begin{pmatrix}k/L_1\\\boldsymbol{\ell}/h\end{pmatrix}\cdot\boldsymbol{S}(k,\boldsymbol{\ell})\right]\begin{pmatrix}k/L_1\\\boldsymbol{\ell}/h\end{pmatrix}\mathrm{e}^{-2\pi\mathrm{i}\begin{pmatrix}k/L_1\\\boldsymbol{\ell}/h\end{pmatrix}\cdot\boldsymbol{x}_j}$$

$$= \frac{8\pi^3\mathrm{i}}{L_1}\sum_{(k,\boldsymbol{\ell})\in\mathcal{I}_{\boldsymbol{M}}}\hat{b}_{|k|,\boldsymbol{\ell}}\begin{pmatrix}k/L_1\\\boldsymbol{\ell}/h\end{pmatrix}\begin{pmatrix}k/L_1\\\boldsymbol{\ell}/h\end{pmatrix}^{\top}\left[\begin{pmatrix}k/L_1\\\boldsymbol{\ell}/h\end{pmatrix}\cdot\boldsymbol{S}(k,\boldsymbol{\ell})\right]\boldsymbol{\mu}_j\mathrm{e}^{-2\pi\mathrm{i}\begin{pmatrix}k/L_1\\\boldsymbol{\ell}/h\end{pmatrix}\cdot\boldsymbol{x}_j}.$$

The efficient computation of the Fourier space parts $\boldsymbol{F}^{1d,F}(j)$ can be done analogously to the 3d-periodic case via Algorithm (2.3) ($\mathrm{i}\boldsymbol{k}$-differentiation) or via Algorithm (2.4) (analytic differentiation), where we make the replacements (4.4) and (4.5).

5 Open boundary conditions

In some applications no periodic boundary conditions are required, i.e., we set $\mathcal{S} := \{0\}^3$ and define the energy U^{0d} by

$$U^{0d} := U_{\{0\}^3} = \frac{1}{2}\sum_{i,j=1}^{N}{}'(\boldsymbol{\mu}_i \cdot \nabla_{\boldsymbol{x}_i})(\boldsymbol{\mu}_j \cdot \nabla_{\boldsymbol{x}_j})\frac{1}{\|\boldsymbol{x}_{ij}\|}.$$

We could compute the energy as well as the fields, torques and forces directly since we only have to compute finite sums, but the computational cost is $\mathcal{O}(N^2)$. In order to enable a more efficient evaluation we apply the splitting (1.7) and obtain

$$U^{0d} = U^{0d,\text{short}} + U^{0d,\text{long}} + U^{\text{self}},$$

where we set

$$U^{0d,\text{short}} := \frac{1}{2}\sum_{i,j=1}^{N}{}'(\boldsymbol{\mu}_i \cdot \nabla_{\boldsymbol{x}_i})(\boldsymbol{\mu}_j \cdot \nabla_{\boldsymbol{x}_j})\frac{\operatorname{erfc}(\alpha\|\boldsymbol{x}_{ij}\|)}{\|\boldsymbol{x}_{ij}\|},$$

$$U^{0d,\text{long}} := \frac{1}{2}\sum_{i,j=1}^{N}(\boldsymbol{\mu}_i \cdot \nabla_{\boldsymbol{x}_i})(\boldsymbol{\mu}_j \cdot \nabla_{\boldsymbol{x}_j})\frac{\operatorname{erf}(\alpha\|\boldsymbol{x}_{ij}\|)}{\|\boldsymbol{x}_{ij}\|},$$

and the self interaction energy is defined in (1.11).

The complementary error function tends to zero very rapidly and thus the short range part can be obtained by only considering small distances $\|\boldsymbol{x}_{ij}\|$ for a reasonable choice of α and the near field cutoff r_{cut}.

We apply the regularization approach, as described for the 1d-periodic case in Section 4, to the kernel function in the long range part

$$\frac{\mathrm{erf}(\alpha\|\boldsymbol{x}_{ij}\|)}{\|\boldsymbol{x}_{ij}\|}.$$

Note, that the periodization of this function is not possible since it does not decrease fast enough.

If the dipoles are distributed in the box $[-L_1/2, L_1/2] \times [-L_2/2, L_2/2] \times [-L_3/2, L_3/2]$ we have $\|\boldsymbol{x}_{ij}\| \leq \sqrt{L_1^2 + L_2^2 + L_3^2}$. For the regularization we choose $h > 2\sqrt{L_1^2 + L_2^2 + L_3^2}$ and construct the interpolating polynomial

$$P : \left[\sqrt{L_1^2 + L_2^2 + L_3^2}, h/2\right] \to \mathbb{R}$$

such that

$$\frac{\mathrm{d}^n}{\mathrm{d}r^n} \frac{\mathrm{erf}(\alpha r)}{r}\bigg|_{r=\sqrt{L_1^2+L_2^2+L_3^2}} = \frac{\mathrm{d}^n}{\mathrm{d}r^n} P(r)\bigg|_{r=\sqrt{L_1^2+L_2^2+L_3^2}}$$

for all $n = 0, \ldots, p$ and

$$\frac{\mathrm{d}^n}{\mathrm{d}r^n} P(r)\bigg|_{r=h/2} = 0$$

for all $n = 1, \ldots, p$. We define the regularization $R \in C^p[-h/2, h/2]^3$ by

$$R(\boldsymbol{y}) := \begin{cases} \dfrac{\mathrm{erf}(\alpha\|\boldsymbol{y}\|)}{\|\boldsymbol{y}\|} & : \|\boldsymbol{y}\| \leq \sqrt{L_1^2 + L_2^2 + L_3^2}, \\ P(\|\boldsymbol{y}\|) & : \sqrt{L_1^2 + L_2^2 + L_3^2} < \|\boldsymbol{y}\| \leq h/2, \\ P(h/2) & : \|\boldsymbol{y}\| > h/2. \end{cases}$$

Now we can approximate the function R by a trivariate trigonometric polynomial

$$R(\boldsymbol{y}) \approx \sum_{\boldsymbol{\ell} \in \mathcal{I}_M} \hat{b}_{\boldsymbol{\ell}} \mathrm{e}^{2\pi\mathrm{i}(\boldsymbol{\ell}/h)\cdot\boldsymbol{y}},$$

where we choose $\boldsymbol{M} \in 2\mathbb{N}^3$ large enough and the Fourier coefficients

$$\hat{b}_{\boldsymbol{\ell}} := \frac{1}{|\mathcal{I}_M|} \sum_{\boldsymbol{j} \in \mathcal{I}_M} R((\boldsymbol{j} \oslash \boldsymbol{M})h) \mathrm{e}^{-2\pi\mathrm{i}(\boldsymbol{j}\oslash\boldsymbol{M})\cdot\boldsymbol{\ell}}$$

can be computed via the FFT after sampling the function R on the equispaced grid $\mathcal{I}_M$.

Inserting the distances of the particles we obtain

$$\frac{\mathrm{erf}(\alpha\|\boldsymbol{x}_{ij}\|)}{\|\boldsymbol{x}_{ij}\|} = R(\|\boldsymbol{x}_{ij}\|) \approx \sum_{\boldsymbol{\ell} \in \mathcal{I}_M} \hat{b}_{\boldsymbol{\ell}} \mathrm{e}^{2\pi\mathrm{i}(\boldsymbol{\ell}/h)\cdot\boldsymbol{x}_{ij}}. \tag{5.1}$$

5.1 Computation of the electrostatic fields and torques

With (1.5) we obtain

$$\boldsymbol{E}^{0\mathrm{d}}(j) = \boldsymbol{E}^{0\mathrm{d},\mathrm{short}}(j) + \boldsymbol{E}^{0\mathrm{d},\mathrm{long}}(j) + \boldsymbol{E}^{\mathrm{self}}(j),$$

where we set

$$\boldsymbol{E}^{0\mathrm{d},\mathrm{short}}(j) := -\nabla_{\boldsymbol{x}_j} \sum_{i=1}^{N}{}' (\boldsymbol{\mu}_i \cdot \nabla_{\boldsymbol{x}_i}) \frac{\mathrm{erfc}(\alpha\|\boldsymbol{x}_{ij}\|)}{\|\boldsymbol{x}_{ij}\|},$$

$$\boldsymbol{E}^{0\mathrm{d},\mathrm{long}}(j) := -\nabla_{\boldsymbol{x}_j} \sum_{i=1}^{N} (\boldsymbol{\mu}_i \cdot \nabla_{\boldsymbol{x}_i}) \frac{\mathrm{erf}(\alpha\|\boldsymbol{x}_{ij}\|)}{\|\boldsymbol{x}_{ij}\|},$$

and the self term $\boldsymbol{E}^{\mathrm{self}}(j)$ is the same as in (2.8).

Inserting the precomputed approximation (5.1) we obtain for the long range parts

$$\boldsymbol{E}^{0\mathrm{d},\mathrm{long}}(j) \approx -\nabla_{\boldsymbol{x}_j} \sum_{\boldsymbol{\ell} \in \mathcal{I}_M} \hat{b}_{\boldsymbol{\ell}} \left(\sum_{i=1}^{N} (\boldsymbol{\mu}_i \cdot \nabla_{\boldsymbol{x}_i}) \mathrm{e}^{2\pi\mathrm{i}(\boldsymbol{\ell}/h)\cdot\boldsymbol{x}_i} \right) \mathrm{e}^{-2\pi\mathrm{i}(\boldsymbol{\ell}/h)\cdot\boldsymbol{x}_j}$$

$$= -4\pi^2 \sum_{\boldsymbol{\ell} \in \mathcal{I}_M} \hat{b}_{\boldsymbol{\ell}}(\boldsymbol{\ell}/h) \left[(\boldsymbol{\ell}/h) \cdot \boldsymbol{S}(\boldsymbol{\ell}) \right] \mathrm{e}^{-2\pi\mathrm{i}(\boldsymbol{\ell}/h)\cdot\boldsymbol{x}_j},$$

where we define

$$\boldsymbol{S}(\boldsymbol{\ell}) := \sum_{i=1}^{N} \boldsymbol{\mu}_i \mathrm{e}^{2\pi\mathrm{i}(\boldsymbol{\ell}/h)\cdot\boldsymbol{x}_i}.$$

The efficient approximation of the long range parts $\boldsymbol{E}^{0\mathrm{d},\mathrm{long}}(j)$ can be done as in the 3d-periodic case via Algorithm (2.1) (i$\boldsymbol{k}$-differentiation) or via Algorithm (2.2) (analytic differentiation), where we formally replace

$$\frac{1}{V}\hat{\psi}(\boldsymbol{k}), \boldsymbol{k} \in \mathcal{I}_M, \quad \text{by} \quad \pi\hat{b}_{\boldsymbol{\ell}}, \boldsymbol{\ell} \in \mathcal{I}_M, \tag{5.2}$$

and

$$\boldsymbol{k} \oslash \boldsymbol{L} \in \mathbb{R}^3 \quad \text{by} \quad (\boldsymbol{\ell}/h) \in \mathbb{R}^3. \tag{5.3}$$

We denote the approximated fields by

$$\boldsymbol{E}_{\approx}^{0\mathrm{d}}(j) \approx \boldsymbol{E}_{\approx}^{0\mathrm{d},\mathrm{short}}(j) + \boldsymbol{E}_{\approx}^{0\mathrm{d},\mathrm{long}}(j) + \boldsymbol{E}^{\mathrm{short}}(j),$$

where the short range parts $\boldsymbol{E}_{\approx}^{0\mathrm{d},\mathrm{short}}(j)$ are obtained by a direct summation.

Based on the computed approximations of the fields $\boldsymbol{E}_{\approx}^{0\mathrm{d}}(j)$ the torques are simply obtained by (1.3), i.e., we approximate the torques by

$$\boldsymbol{\tau}^{0\mathrm{d}}(j) \approx \boldsymbol{\tau}_{\approx}^{0\mathrm{d}}(j) := \boldsymbol{\mu}_j \times \boldsymbol{E}_{\approx}^{0\mathrm{d}}(j).$$

An approximation of the energy $U^{0\mathrm{d}}$ is given by

$$U_{\approx}^{0\mathrm{d}} := -\frac{1}{2} \sum_{j=1}^{N} \boldsymbol{\mu}_j \cdot \boldsymbol{E}_{\approx}^{0\mathrm{d}}(j),$$

following the identity (1.5).

5.2 Computation of the forces

We rewrite the forces in the 0d-periodic case as

$$\boldsymbol{F}^{\mathrm{0d}}(j) = \nabla_{\boldsymbol{x}_j}\left[\boldsymbol{\mu}_j \cdot \boldsymbol{E}^{\mathrm{0d}}(j)\right] = \boldsymbol{F}^{\mathrm{0d,short}}(j) + \boldsymbol{F}^{\mathrm{0d,long}}(j),$$

where we set $\boldsymbol{F}^{\mathrm{0d,short}}(j) := \boldsymbol{F}^{\mathrm{short}}_{\{0\}^3}(j)$ via (2.10) and for the long range part we obtain

$$
\begin{aligned}
\boldsymbol{F}^{\mathrm{0d,long}}(j) &= -\nabla_{\boldsymbol{x}_j}(\boldsymbol{\mu}_j \cdot \nabla_{\boldsymbol{x}_j})\sum_{i=1}^{N}(\boldsymbol{\mu}_i \cdot \nabla_{\boldsymbol{x}_i})\frac{\mathrm{erf}(\alpha\|\boldsymbol{x}_{ij}\|)}{\|\boldsymbol{x}_{ij}\|} \\
&\approx -\nabla_{\boldsymbol{x}_j}(\boldsymbol{\mu}_j \cdot \nabla_{\boldsymbol{x}_j})\sum_{\boldsymbol{\ell}\in\mathcal{I}_M}\hat{b}_{\boldsymbol{\ell}}\left(\sum_{i=1}^{N}(\boldsymbol{\mu}_i \cdot \nabla_{\boldsymbol{x}_i})\mathrm{e}^{2\pi\mathrm{i}(\boldsymbol{\ell}/h)\cdot\boldsymbol{x}_i}\right)\mathrm{e}^{-2\pi\mathrm{i}(\boldsymbol{\ell}/h)\cdot\boldsymbol{x}_j} \\
&= 8\pi^3\mathrm{i}\sum_{\boldsymbol{\ell}\in\mathcal{I}_M}\hat{b}_{\boldsymbol{\ell}}\left[\boldsymbol{\mu}_j\cdot(\boldsymbol{\ell}/h)\right]\left[(\boldsymbol{\ell}/h)\cdot\boldsymbol{S}(\boldsymbol{\ell})\right](\boldsymbol{\ell}/h)\mathrm{e}^{-2\pi\mathrm{i}(\boldsymbol{\ell}/h)\cdot\boldsymbol{x}_j} \\
&= 8\pi^3\mathrm{i}\sum_{\boldsymbol{\ell}\in\mathcal{I}_M}\hat{b}_{\boldsymbol{\ell}}(\boldsymbol{\ell}/h)(\boldsymbol{\ell}/h)^{\top}\left[(\boldsymbol{\ell}/h)\cdot\boldsymbol{S}(\boldsymbol{\ell})\right]\boldsymbol{\mu}_j\mathrm{e}^{-2\pi\mathrm{i}(\boldsymbol{\ell}/h)\cdot\boldsymbol{x}_j}.
\end{aligned}
$$

The efficient computation of the long range parts $\boldsymbol{F}^{\mathrm{0d,long}}(j)$ can be done analogously to the 3d-periodic case via Algorithm (2.3) ($\mathrm{i}\boldsymbol{k}$-differentiation) or via Algorithm (2.4) (analytic differentiation), where we make the replacements (5.2) and (5.3).

6 Summary

In this paper we presented an NFFT based approach to the efficient computation of dipole-dipole interactions. For 3d-periodic boundary conditions the presented method is very similar to the well known P^{3}M method for dipolar systems [6]. We considered for the first time also mixed periodic boundary conditions as well as open boundary conditions, for which the final algorithms are completely of the same structure as for 3d-periodic constraints. Thereby, we considered the well known $\mathrm{i}\boldsymbol{k}$-differentiation as well as the analytical differentiation approach in order to compute the electrostatic fields and the acting forces.

For mixed periodic as well as open boundary conditions the Fourier coefficients are not known analytically, in contrast to the 3d-periodic case, and the contributions in the nonperiodic dimensions have at first to be approximated by trigonometric polynomials before fast Fourier transforms can be applied. This is done in a precomputation step, which has to be done only once if the particles do not leave the initial simulation box.

The same idea has already been applied successfully to the computation of Coulomb interactions in point charges systems under all considered types of periodic boundary conditions, see [25, 26]. The method has already been implemented and is part of the publicly available ScaFaCoS library [2]. In this paper we showed that the algorithms can be generalized to the computation of dipole-dipole interactions. The implementation as well as the testing of the method is subject of ongoing research. Numerical results will be published in a future paper.

Acknowledgments

References

[1] R.P. Agarwal and P.J.Y. Wong: *Error inequalities in polynomial interpolation and their applications*, vol. 262 of *Mathematics and its Applications*. Kluwer Academic Publishers Group, Dordrecht, 1993.

[2] A. Arnold, M. Bolten, H. Dachsel, F. Fahrenberger, F. Gähler, R. Halver, F. Heber, M. Hofmann, J. Iseringhausen, I. Kabadshow, O. Lenz, and M. Pippig: *ScaFaCoS - Scalable Fast Coloumb Solvers*. http://www.scafacos.de.

[3] A. Arnold, F. Fahrenberger, C. Holm, O. Lenz, M. Bolten, H. Dachsel, R. Halver, I. Kabadshow, F. Gähler, F. Heber, J. Iseringhausen, M. Hofmann, M. Pippig, D. Potts, and G. Sutmann: *Comparison of scalable fast methods for long-range interactions*. Phys. Rev. E, 88:063308, 2013.

[4] G. Beylkin: *On the fast Fourier transform of functions with singularities*. Appl. Comput. Harmon. Anal., 2:363 – 381, 1995.

[5] J.J. Cerdà, V. Ballenegger, and C. Holm: *Particle-particle particle-mesh method for dipolar interactions: On error estimates and efficiency of schemes with analytical differentiation and mesh interlacing*. J. Chem. Phys., 135:184110, 2011.

[6] J.J. Cerdà, V. Ballenegger, O. Lenz, and C. Holm: *P3M algorithm for dipolar interactions*. J. Chem. Phys., 129:234104, 2008.

[7] T. Darden, D. York, and L. Pedersen: *Particle mesh Ewald: An $n \log(n)$ method for Ewald sums in large systems*. J. Chem. Phys., 98:10089–10092, 1993.

[8] M. Deserno and C. Holm: *How to mesh up Ewald sums. I. A theoretical and numerical comparison of various particle mesh routines*. J. Chem. Phys., 109:7678 – 7693, 1998.

[9] M. Deserno and C. Holm: *How to mesh up Ewald sums. II. An accurate error estimate for the Particle-Particle-Particle-Mesh algorithm*. J. Chem. Phys., 109:7694 – 7701, 1998.

[10] A. Dutt and V. Rokhlin: *Fast Fourier transforms for nonequispaced data*. SIAM J. Sci. Stat. Comput., 14:1368 – 1393, 1993.

[11] U. Essmann, L. Perera, M.L. Berkowitz, T. Darden, H. Lee, and L.G. Pedersen: *A smooth particle mesh Ewald method*. J. Chem. Phys., 103:8577 – 8593, 1995.

[12] P.P. Ewald: *Die Berechnung optischer und elektrostatischer Gitterpotentiale*. Ann. Phys., 369:253–287, 1921.

[13] M. Fenn and G. Steidl: *Fast NFFT based summation of radial functions*. Sampl. Theory Signal Image Process., 3:1 – 28, 2004.

[14] D. Frenkel and B. Smit: *Understanding molecular simulation: From algorithms to applications*. Academic Press, 2002.

[15] L. Greengard and J.Y. Lee: *Accelerating the nonuniform fast Fourier transform*. SIAM Rev., 46:443 – 454, 2004.

[16] A. Grzybowski, E. Gwóźdź, and A. Bródka: *Ewald summation of electrostatic interactions in molecular dynamics of a three-dimensional system with periodicity in two directions.* Phys. Rev. B, 61:6706–6712, 2000.

[17] F.E. Harris: *Incomplete Bessel, generalized incomplete gamma, or leaky aquifer functions.* J. Comput. Appl. Math., 215:260 – 269, 2008.

[18] R.W. Hockney and J.W. Eastwood: *Computer simulation using particles.* Taylor & Francis, Inc., Bristol, PA, USA, 1988.

[19] J. Keiner, S. Kunis, and D. Potts: *Using NFFT3 - a software library for various non-equispaced fast Fourier transforms.* ACM Trans. Math. Software, 36:Article 19, 1 – 30, 2009.

[20] S.W. de Leeuw, J.W. Perram, and E.R. Smith: *Simulation of electrostatic systems in periodic boundary conditions. I. Lattice sums and dielectric constants.* Proc. R. Soc. Lond. Ser. A Math. Phys. Eng. Sci., 373:27 – 56, 1980.

[21] D. Lindbo and A.K. Tornberg: *Spectral accuracy in fast Ewald-based methods for particle simulations.* J. Comput. Phys., 230:8744 – 8761, 2011.

[22] D. Lindbo and A.K. Tornberg: *Fast and spectrally accurate Ewald summation for 2-periodic electrostatic systems.* J. Chem. Phys., 136:164111, 2012.

[23] F. Nestler: *Parameter tuning for the NFFT based fast Ewald summation.* Preprint 2015-05, Faculty of Mathematics, Technische Universität Chemnitz, 2015.

[24] F. Nestler: *Automated parameter tuning based on RMS errors for nonequispaced FFTs.* Adv. Comput. Math., 2015, accepted.

[25] F. Nestler, M. Pippig, and D. Potts: *Fast Ewald summation based on NFFT with mixed periodicity.* J. Comput. Phys., 285:280 – 315, 2015.

[26] F. Nestler, M. Pippig, and D. Potts: *NFFT based fast Ewald summation for various types of periodic boundary conditions.* In G. Sutmann, J. Grotendorst, G. Gompper, and D. Marx (eds.): *Computational Trends in Solvation and Transport in Liquids*, vol. 28 of *IAS-Series*, pp. 575 – 598, Jülich, 2015. Forschungszentrum Jülich GmbH.

[27] M. Pippig and D. Potts: *Particle simulation based on nonequispaced fast Fourier transforms.* In G. Sutmann, P. Gibbon, and T. Lippert (eds.): *Fast Methods for Long-Range Interactions in Complex Systems*, vol. 6 of *IAS-Series*, pp. 131 – 158, Jülich, 2011. Forschungszentrum Jülich GmbH.

[28] M. Pippig and D. Potts: *Parallel three-dimensional nonequispaced fast Fourier transforms and their application to particle simulation.* SIAM J. Sci. Comput., 35:C411 – C437, 2013.

[29] M. Porto: *Ewald summation of electrostatic interactions of systems with finite extent in two of three dimensions.* J. Phys. A, 33:6211 – 6218, 2000.

[30] D. Potts, G. Steidl, and M. Tasche: *Fast Fourier transforms for nonequispaced data: A tutorial.* In J.J. Benedetto and P.J.S.G. Ferreira (eds.): *Modern Sampling Theory: Mathematics and Applications*, pp. 247 – 270, Boston, MA, USA, 2001. Birkhäuser.

[31] R.M. Slevinsky and H. Safouhi: *A recursive algorithm for the G transformation and accurate computation of incomplete Bessel functions.* Appl. Numer. Math., 60:1411 – 1417, 2010.

[32] G. Steidl: *A note on fast Fourier transforms for nonequispaced grids.* Adv. Comput. Math., 9:337 – 353, 1998.

[33] A.F. Ware: *Fast approximate Fourier transforms for irregularly spaced data.* SIAM Rev., 40:838 – 856, 1998.